333
7/17/79

H. 2866

ORNL-5526

MASTER

Effects of Temperature, Temperature Gradients, Stress, and Irradiation on Migration of Brine Inclusions in a Salt Repository

G. H. Jenks

BLANK PAGE

ORNL-5526
Dist. Category UC-70

/

Contract No. W-7405-eng-26

CHEMICAL TECHNOLOGY DIVISION

EFFECTS OF TEMPERATURE, TEMPERATURE GRADIENTS, STRESS, AND IRRADIATION ON MIGRATION OF BRINE INCLUSIONS IN A SALT REPOSITORY

G. H. Jenks

With an Appendix by C. F. Baes, Jr., and R. W. Gable*

Date Published: July 1979

*Associate Professor of Chemistry, Davidson College, Davidson, N.C.; presently a visiting member of the ORNL Chemistry Division.

The project was administered by the Office of Nuclear Waste Isolation, Battelle Memorial Institute.

OAK RIDGE NATIONAL LABORATORY
Oak Ridge, Tennessee 37830
operated by
UNION CARBIDE CORPORATION
for the
DEPARTMENT OF ENERGY

CONTENTS

EFFECTS OF TEMPERATURE, TEMPERATURE GRADIENTS, STRESS, AND IRRADIATION ON MIGRATION OF BRINE INCLUSIONS IN A SALT REPOSITORY

G. H. Jenks

ABSTRACT

This report reviews and analyzes available experimental and theoretical information on brine migration in bedded salt. The effects of temperature, thermal gradients, stress, irradiation, and pressure in a salt repository are among the factors considered.

The theoretical and experimental (with results of Anthony and Cline were used to correlate and explain the ailable data for rates of brine migration at temperatures up to 250°C in naturally occurring crystals of bedded salt from Lyons and Hutchinson, Kansas. It was concluded that the following empirical equation for V/G_s (migration velocity of brine inclusion per unit temperature gradient in the salt) represents the maximum values for this parameter which would result from thermal gradients in the bedded salt crystals in a repository:

$$\log V/G_s = 0.00656T - 0.6036,$$

where T is the temperature of the salt (°C), and V/G_s has the units (cm^2 $year^{-1}$ $°C^{-1}$).

Considerations of the effects of stressing crystals of bedded salt on the migration properties of brine inclusions within the crystals led to the conclusion that the most probable effects are a small fractional increase in the solubility of the salt within the liquid and a concomitant and equal fractional increase in the rate of the thermal gradient-induced migration of the brine. The application of high pressure could reduce the value of the kinetic potential from that prevailing in the absence of the pressure, but this would not affect the maximum rates predicted by the equation shown above.

The presence of stored radiation energy within a salt crystal could affect the rate of brine migration within the crystal if the stored energy causes an increase in the solubility of the salt. However, results obtained in Project Salt Vault suggested that stored radiation energy had little, if any, influence on the rate of brine flow into the emplacement cavities in the salt. No direct information regarding the effect of stored energy on the solubility of salt is available; thus I recommend that experiments be undertaken to provide such information.

The greatest uncertainty relative to the prediction of rates of migration of brine into a waste emplacement cavity in bedded salt is associated with questions concerning the effects of the grain boundaries (within the aggregates of single crystals which comprise a bedded salt deposit) on brine migration through the deposit. It is likely that the grain boundary trapping will tend to retard brine migration under the conditions expected to prevail with probable repository designs (viz., $G_s \leq 2°C$ maximum, impurities present on grain boundaries, and boundaries compressed by thermal expansion of the salt).

The results of some of the estimates of rates and total amounts of brine inflow to HLW and SURF waste packages emplaced in bedded salt were included to illustrate the inflow volumes which might occur in a repository. These estimates, which are based on the results of temperature calculations reported by others, employed the assumptions that (1) the salt contained 0.5 vol % brine inclusions, (2) these inclusions migrated at the maximum rates shown by the equation presented earlier, and (3) grain boundaries had no effect on the migration.

The results of the brine inflow estimates for 10-year-old HLW emplaced at 150 kW/acre indicated inflow rates starting at 0.7 liter/year and totaling 12 liters at 30 years after emplacement. (Temperature calculations did not extend beyond 35 years.)

The results of the estimates for 10-year-old PWR SURF emplaced at 60 kW/acre indicated a constant inflow of 0.035 liter/year for the first 35 years after emplacement. (Temperature calculations did not extend beyond 35 years.)

---

1. INTRODUCTION

Bedded salt usually contains a small volume fraction of brine inclusions, some of which are located within the small crystals that comprise the salt deposits. These inclusions can migrate through the salt under conditions where a sufficiently large gradient exists in the chemical potential of the salt around the inclusions. Both theoretical considerations and experimental results have established that temperature gradients cause brine-filled cavities within the salt to migrate up the temperature gradient. No comparable theoretical or experimental information has been reported for the other factors that might affect chemical potentials in the salt.

Data relative to the rates and total amounts of brine migration to a waste package within a salt repository are, of course, needed in evaluating the feasibility and suitability of a given disposal concept. The quantitative, as well as the qualitative, effects of brine migration on the repository are now under discussion in the scientific community. Questions have been raised as to what influence stress, plastic flow, and other factors may have on the rates and amounts of migrating brine.

Available experimental and theoretical information on thermal gradient-induced brine migration in bedded salt has been reviewed, and the results are presented here. Available information bearing on the effects of other parameters on brine migration has also been reviewed and analyzed. The thermal-gradient information has been used as an aid and criterion in estimating the effects of the other parameters on brine migration in a repository.

2. DESCRIPTION OF BRINE INCLUSIONS

Bedded salt from the Lyons, Kansas, area* is comprised of closely bound aggregates of irregularly shaped single crystals. The characteristic dimensions of these crystals range from ∿0.3 to 3 cm.[1-3] Brine inclusions (droplets) can be observed within the single crystals in hand specimens.[2-4] The dimensions of these droplets range from very small to >1 mm.[2-4] Most of the brine volume is probably contained within the larger droplets (i.e., those greater than ∿0.5 mm). Cursory examinations of hand specimens of bedded salt from Detroit, Michigan, and from AEC Cores 7 and 8 from New Mexico have indicated that the crystal sizes and the aggregates are similar to those from Lyons. Also, brine inclusions were present in these specimens from other salt deposits.

Many of the larger droplets in the Lyons salt exhibit a low-pressure gas vapor bubble when examined at temperatures near those which prevailed in the salt formation, ∿25°C at a depth of ∿1000 ft.[5] These bubbles,

---

*Carey and American Salt Company Mines are located at Lyons, Kansas. Carey and other mines are located at Hutchinson, Kansas.

which generally occupied a few percent of the inclusion volume,[4] disappeared on heating the crystal to 80 to 100°C.[4] Low-pressure bubbles were also reported in samples of New Mexico salt obtained from ERDA Core 9 at depths of 1800 to 2800 ft, but they disappeared on heating to temperatures between 20.4 and 45.5°C.[6] The occurrence of those bubbles in New Mexico salt that disappeared below ∿30 to 35°C can probably be explained on the basis of the maximum temperatures prevailing in the undisturbed geologic formation at the depths from which the cores were taken. However, the occurrence of those bubbles that persisted to higher temperaures in the samples from New Mexico and from Lyons has not been explained. It seems unlikely the low-pressure bubbles could exist under natural in-place conditions because of the plastic creep of the salt at the high overburden pressures (∿1000 psi at Lyons and up to ∿2800 psi at New Mexico) over very long times. The possibility that the bubbles were formed after the salt was extracted from the formation has not been completely ruled out.

Chemical analyses[5,7] of encapsulated brine in bedded salt from Lyons, Kansas, and from nearby (∿20 miles) Hutchinson, Kansas, showed ∿2.1 M $MgCl_2$ and ∿1.9 M NaCl. Small amounts of calcium, bromine, SO_4^{2-} and, probably, potassium were also present. No direct analyses of encapsulated brine from other salt deposits have been reported. However, analytical results for salt samples taken from cores AEC 7 and 8, from locations near the WIPP site in New Mexico, indicate that the composition of any encapsulated brine within the samples was similar to that of brine in the Kansas salt. The composition of encapsulated brine in bedded salt is discussed in Appendix A.

3. THERMAL GRADIENT-INDUCED BRINE MIGRATION IN BEDDED SALT

3.1 Theoretical

Wilcox[8,9] was the first to report a theoretical analysis of brine migration in NaCl. His work included a study of the influence of temperature on the rate of migration. Shortly afterward, Bradshaw and Sanchez,[10]

working independently, also reported a theoretical analysis of brine migration in NaCl induced by the thermal gradient. A theoretical relationship was developed for the migration rate of a brine inclusion as a function of the temperature gradient and temperature. More recently, Anthony and Cline[11-16] published several papers dealing with their experimental and theoretical work on brine migration in KCl. Wilcox et al.[17,18] also published other work dealing with brine migration in NaCl. The theoretical analysis of Anthony and Cline, which is more complete than that of either Bradshaw and Sanchez or Wilcox et al., is also applicable to NaCl. Accordingly, the work of Anthony and Cline was of primary interest in the present study.

The thermomigration of a brine droplet up a temperature gradient results from an increase in the solubility of the salt with increased temperature and/or from thermal diffusion effects within the brine (i.e., from the Soret effect). The velocity of droplet migration depends on droplet size, as well as on several other parameters (including those just mentioned). The migration can also be affected by grain boundaries.[13]

The theoretical expression of Anthony and Cline[11,13] for the migration velocity of droplets within the body of a crystal is given by the first three terms in Eq. (1):

$$V = \frac{C_\ell}{C_s}\frac{D}{RT}\left[\left(\frac{1}{C_\ell}\frac{\partial C_E}{\partial T} - \sigma\right)G_\ell RT - \frac{K}{L} - \frac{4\gamma\bar{V}_s}{XL}\right], \qquad (1)$$

where

V = migration velocity, cm/sec;

C_ℓ = concentration of salt in brine droplet, moles/liter;

C_E = equilibrium concentration of salt in brine in contact with salt, moles/liter;

C_s = concentration of salt in solid salt, moles/liter;

D = diffusivity of salt in brine, cm^2/sec;

R = gas constant, ergs $mole^{-1}$ $°C^{-1}$;

T = absolute temperature, °K;

K = kinetic potential, ergs/mole;

γ = grain boundary tension, $ergs/cm^2$;

L = dimension of droplet parallel to thermal gradient, cm;

X = dimension of droplet perpendicular to thermal gradient, cm;

$\bar{V}_s$ = molar volume of solid salt, cm^3/mole;

G_ℓ = temperature gradient in the brine droplet, °C/cm;

σ = Soret coefficient of salt in brine, $°C^{-1}$.*

The final term in this equation involves grain boundary tension, γ, and applies only at grain boundaries.

The temperature gradient within the solution, G_ℓ, at a central location, was related by Anthony and Cline[11] to the gradient within the salt, G_s, as shown in Eq. (2):

$$G_\ell = \frac{k_s G_s}{(1 - F)k_s + Fk_\ell}, \qquad (2)$$

where k_s and k_ℓ are the thermal conductivities of the solid and liquid, respectively, and F is analogous to a demagnetization factor, described and tabulated by Stoner,[11,19] which depends only on the aspect ratio of the droplet. The value of F, which is 0.333 at $X/L = 1$ (cube and sphere), increases to a value of 1 at $X/L \gg 1$ (i.e., for a slab). Intermediate values of F are 0.53, 0.64, and 0.70 at $X/L = 2.0$, 3.0, and 4.0, respectively. Tiller[20] also reported theoretical relationships between G_ℓ and G_s for spheres, cylinders, and slabs of one material embedded in another. His relationships for the sphere and slab are the same as those shown by Eq. (2) using Stoner's values for F. The value of k_s/k_ℓ for brine inclusions within NaCl ranges downward with increasing temperature from ∿8 at 50°C to ∿4.5 at 200°C. Corresponding calculated values of G_ℓ/G_s at $X/L = 1.0$ range from 1.41 at 50°C to 1.35 at 200°C. At $X/L = 2.0$, the values of G_ℓ/G_s range from 1.86 at 50°C to 1.71 at 200°C; at $X/L \gg 1$, they range from 7.9 at 50°C to 4.6 at 200°C.

These calculated values illustrate that the value of G_ℓ/G_s in NaCl changes markedly with the aspect ratio of a brine inclusion and, at high values of X/L, also with temperature.

---

*The sign-convention for the Soret coefficient used by Anthony and Cline was the opposite of that commonly used. Therefore, the sign in their equation has been changed to correspond to the common usage.

The last two terms in Eq. (1) are functions of the size of the brine inclusion and other factors which are discussed later. If the last two terms are ignored for the present, and G_ℓ is replaced with 1.4 G_s, Eq. (1) becomes:

$$V/G_s = 1.4 \frac{C_\ell}{C_s} D\left(\frac{1}{C_\ell} \frac{\partial C_E}{\partial T} - \sigma\right). \tag{3}$$

This expression is somewhat similar to that of Bradshaw and Sanchez.[10] The remaining differences are shown by the following ratio:

$$\frac{V(\text{Anthony, Cline})}{V(\text{Bradshaw, Sanchez})} = \frac{C'_\ell}{C'_s} \left[1 - C_\ell \sigma/(dC_E/dT)\right],$$

where the primes indicate molal concentrations.

As indicated above, the theoretical basis for Eq. (3) was discussed by Anthony and Cline.[11,13] I will not review their derivation except to note that Eq. (3) can be derived from Eqs. (4) and (5),

$$V = J/C_s \tag{4}$$

$$J = -D\nabla C_\ell + D\sigma C_\ell \nabla T_\ell, \tag{5}$$

if it is assumed that the concentrations of salt in solution at the hot and cold interfaces are equal to the equilibrium concentrations at the respective temperatures. Equation (4), in which J is the flux of salt through the brine in a direction parallel to the temperature gradient, ∇T_ℓ, results from material balance considerations. Equation (5) states the relationship between the flux and the gradients of concentration, ∇C_ℓ, and of temperature, ∇T_ℓ; $D\sigma$ is the thermal diffusion coefficient.

Table 1 lists the values of V/G_s for brine inclusions in Kansas salt which were estimated for the temperature range 50 to 200°C using Eq. (3). The values for the various parameters used in making these estimates are also included, and their sources are identified in the footnotes. No pressure effects other than saturation vapor pressures

Table 1. Theoretical and experimental values for rates of thermal gradient-induced brine migration at 50 to 200°C, and values for parameters in Eq. (3) used in theoretical calculations[a]

Temperature (°C)	C_ℓ/C_s[b]	$\frac{1}{C_\ell}\frac{\partial C_E}{\partial T}$ ($°C^{-1}$)[c]	D (cm^2/sec)[d]	Values of V/G_s (10^{-8} cm^2 sec^{-1} $°C^{-1}$) [cm^2 $year^{-1}$ $°C^{-1}$] Calculated using assumed values for σ as shown[e]				
				0	-0.002	-0.003	-0.004	Experimental[f]
50	0.0549	3.23×10^{-3}	3.2×10^{-5}	0.80 [0.25]	1.28 [0.47]	1.53 [0.49]	1.77 [0.56]	1.68 [0.53]
100	0.0634	3.36×10^{-3}	7.1×10^{-5}	2.12 [0.67]	3.38 [1.06]	4.01 [1.26]	4.64 [1.46]	3.56 [1.12]
150	0.0732	3.85×10^{-3}	12.5×10^{-5}	4.93 [1.55]	7.49 [2.36]	8.77 [2.76]	10.1 [3.19]	7.62 [2.40]
200	0.0836	3.78×10^{-3}	19.9×10^{-5}	8.80 [2.77]	13.5 [4.24]	15.8 [4.97]	18.1 [5.71]	16.2 [5.10]

[a] $G_\ell = 1.4\ G_s$.

[b] As discussed and listed in Appendix C.

[c] As discussed and listed in Appendix B. It is assumed that $C_E = C_\ell$.

[d] Estimated using the relationship DT/n = constant. The viscosity, n, of the solutions was assumed to be directly proportional to the viscosity of water. Calculations were made starting with values for D and for n in NaCl solutions near room temperature.

[e] The reported experimental value of σ in concentrated NaCl solutions at 30 to 50°C is about $-0.002°C^{-1}$.[21-23] No reported experimental or theoretical values were found either for higher temperatures in NaCl solutions or for the $MgCl_2$-rich solutions that occur as brine inclusions.

[f] Values given by the relationship between V/G_s and T which was deduced by Jenks[24] as a conservative representation of the experimental values of Bradshaw and Sanchez.[10]

were considered in the calculations. Pressure and stress effects are discussed in Sect. 4.

The values calculated for V/G_s are compared with those determined experimentally in Sect. 3.3. However, it is worth noting here that a principal factor in the increase in the calculated value with temperature is the increase in the value of the diffusion coefficient. Also, plausible values for the Soret coefficient, σ, indicate that the effects of thermal diffusion on brine migration rates might be roughly equivalent to those resulting from solubility changes with temperature.

The final two terms in Eq. (1) will now be considered. According to Anthony and Cline,[15,16] a frictional force represented by K/L can significantly affect the migration in salt of all droplets. The term K, which designates the kinetic potential, represents the change in chemical potential generated by irreversible processes associated with the transfer of ions between the solid and liquid phases.

The values of K are representative of the undersaturation and supersaturation required at the dissolving and depositing interfaces, respectively, in order for these processes to occur at rates sufficient to support the rate of migration of the droplet. Values of K as a function of brine droplet velocity in KCl at room temperature were reported by Cline and Anthony[15] for accelerational as well as thermal fields. The values of K and V were linearly related, at least up to 1×10^{-7} cm/sec, according to the general equation

$$K = \beta V + b. \tag{6}$$

For their reported results in accelerational fields (V ranged up to 5×10^{-8} cm/sec), calculations show that $\beta = 1.85 \times 10^{14}$ erg-sec mole^{-1} cm^{-1} and $b = 2.0 \times 10^{6}$ ergs/mole. Approximately the same values are found for their thermal field results at V up to $\sim 1 \times 10^{-7}$ cm/sec. Above $\sim 1 \times 10^{-7}$ cm/sec, the values of K were increasing but at less than the rate predicted by the linear relationship. These experimental values in the thermal fields extended to velocities of $\sim 5 \times 10^{-7}$ cm/sec.

The maximum theoretical velocity, V_{max}, for the rate of brine migration within a crystal is the velocity prevailing when K/L is much less than the sum of the other quantities within brackets in Eq. (1). [In this report, the grain boundary term in Eq. (1) is omitted from the considerations of brine migration within a crystal.] With this understanding, Eq. (7) is used to evaluate the ratio V/V_{max} and Eq. (8) gives another relationship between K and the ratio V/V_{max}:

$$V/V_{max} = 1 - \left(\frac{K}{L}\right) \frac{1}{\left(\frac{1}{C_\ell}\frac{\partial C_E}{\partial T} - \sigma\right) G_\ell RT} \tag{7}$$

and

$$K = L\left(1 - \frac{V}{V_{max}}\right)\left(\frac{1}{C_\ell}\frac{\partial C_E}{\partial T} - \sigma\right) G_\ell RT. \tag{8}$$

These equations will be used in subsequent discussions of available experimental information on migration of brine inclusions in Kansas salt.

It can be noted here that the influence of the kinetic potential can lead to a flattening of a migrating droplet perpendicular to the thermal gradient. This flattening results in an increase in the ratio of G_ℓ/G_s and a decrease in the value of L. Both of these changes affect the velocity of the droplet at a given value of G_s. Experimental evidence bearing on effects of the kinetic potential with migration of brine inclusions in Kansas salt is discussed in Sect. 3.3.

The breakup of large droplets in KCl in the presence of a thermal gradient at room temperature was also reported by Anthony and Cline.[16] This breakup was a result of differences between the thermal gradients in the center and at the edges of a droplet. Droplets with a velocity-to-thermal-gradient ratio less than 9.4×10^{-8} cm^2/sec·°C were stable, while those with a greater ratio were unstable. Experimental evidence bearing on this effect in Kansas salt will be examined in Sect. 3.3.

Another force affecting the motion of small droplets occurs at grain boundaries. As pointed out by Anthony and Cline,[13] droplets on

grain boundaries are in positions of minimum energy; therefore, the thermal-gradient driving force required to propel a droplet across a grain boundary exceeds that for motion through the body of a crystal. Their theoretical expression for the effects of the grain boundary tension force is given by the final term in Eq. (1) (see Sect. 3.1).

No direct information is available on the value for the grain boundary tension prevailing in bedded salt aggregates. However, it will probably be in the neighborhood of 30% of the surface energy for the tilt and twist boundaries which exist between the crystals, assuming that the boundaries are free of impurities.[13,25] The theoretically calculated surface energy of NaCl is a minimum ($\sim$150 ergs/cm^2) on the 100 surfaces and a maximum ($\sim$400 ergs/cm^2) on the 110 surfaces.[26] Accordingly, it is likely that the grain boundary tension in the bedded salt will range between about 50 and 150 ergs/cm^2 for clean boundaries.

The possible importance of this grain boundary term can be judged by comparisons between values for this term and that for the sum of the first two terms within brackets in Eq. (1). When the sum of these three terms is zero or negative, the droplet would be trapped on the grain boundary regardless of the value of K/L. The expression that results from setting the sum of these three terms equal to zero and solving for the product, $G_\ell \cdot X \cdot L$, is as follows:

$$G_\ell \cdot X \cdot L = \frac{4\gamma \bar{V}_s}{\left(\frac{1}{C_\ell}\frac{\partial C_E}{\partial T} - \sigma\right)RT} . \qquad (9)$$

Values for the several different quantities appearing on the right side of Eq. (9) are known or have been estimated for temperatures of interest; thus we can obtain estimates of the value of $G_\ell \cdot X \cdot L$. This term, of course, represents the relationship between the dimensions of a droplet on a grain boundary and the minimum temperature gradient required to move the droplet across the grain boundary.

For illustrative purposes, let us evaluate the right side of Eq. (9) at 100°C by letting $[(1/C_\ell)/(\partial C_E/\partial T)] = 3.5 \times 10^{-3}$ °C^{-1} (as listed

in Table 1), γ = 150 ergs/cm^2 (discussed in a preceding paragraph), and σ = -0.002/°C (discussed earlier in this section and also in Sect. 3.3.2). The molar volume of the solid salt, $\bar{V}_s$, is equal to 27.0 cm^3/mole (Appendix D). Substituting these values into Eq. (9) yields:

$$G_\ell \cdot \Sigma \cdot L = \frac{(4)(150)(27)}{(5.5 \times 10^{-3})(8.31 \times 10^7)(373)} = 9.5 \times 10^{-5}, \quad °C \cdot cm. \qquad (10)$$

When G_ℓ = 1°C/cm, the value of XL in Eq. (10) is 9.5 x 10^{-5} cm^2 and the droplet (assumed to be cubical) would have an edge dimension of 9.7 x 10^{-3} cm. Then, according to the discussion and assumptions made thus far, a cubical droplet with edge $\leq$ 9.7 x 10^{-3} cm would be trapped on a grain boundary unless the value of G_ℓ exceeds 1°C/cm (or, since the droplet is cubical, unless G_s exceeds 0.7°C/cm). The value of G_ℓ required to propel a cubical droplet across a grain boundary is inversely proportional to the square of its edge dimension; in the above example, the required value of G_ℓ would exceed 3.5°C/cm when the edge dimension is $\sim$5 x 10^{-3} cm.

There is some evidence[2,3] that droplets undergo a change in shape and, possibly, size when they reach a grain boundary in bedded salt. Such changes could alter the brine trapping effects on the grain boundary. Also, the presence of impurities on a grain boundary could affect the trapping. Relatively insoluble impurities could prohibit movement across or along grain boundaries; on the other hand, they could also cause the temperature gradient across the boundary to be greater than that within the adjacent crystal and thus promote movement of a droplet across the boundary.

It is evident that a great deal of uncertainty is associated with attempts to theoretically predict the effects of grain boundaries on brine migration in a waste repository in bedded salt. However, it is conceivable that grain boundary trapping will tend to retard brine migration under the conditions expected to prevail with probable repository designs (viz., $G_s \leq$ 2°C/cm maximum,[27] impurities present on grain boundaries, and boundaries compressed by thermal expansion of the salt). It is also conceivable that the effects of grain boundaries will be

opposite to those suggested above under some circumstances (e.g., when salt which has been heated is allowed to cool).

3.2 Experimental

3.2.1 Project Salt Vault

Project Salt Vault[28] was conducted in the Carey Mine at Lyons, Kansas. The experiment included two different arrays of seven heated canisters; one was located in Room 1 and the other in Room 4. Each canister in Room 1 was supplied with a radiation source consisting of spent fuel elements from the ETR. Part of the heat to a given canister was supplied by the radioactive decay heat of the elements; the remainder was obtained from electrical heaters. The array in Room 4 was regarded as an unirradiated control, and electrical heat was supplied to each canister to match the total in the irradiation canisters.

Each canister was arranged in the salt in such a manner that an air gap existed between the canister sleeve and the salt wall. During normal operations, mine air was pulled successively through this gap and a condenser which was cooled to mine air temperature. Provisions were made to collect and measure any liquid water formed within the condenser. (A common condenser was used for the seven heated canisters within an array in a given room.) It was observed that water was collected only during or immediately after a failure of electrical power during which salt adjacent to a canister cooled to some extent. The amount of water collected during the first 2 days after shutdown of the heaters at the end of the experiment was about ten times greater than that collected during the entire prior period of operation, 580 days.

Details of the complete experiment, along with the results and conclusions are presented in ref. 28. However, for convenience, information which is available, or which can be inferred from ref. 28, and has a possible bearing on brine migration considerations is assembled in Table 2. (It should be added that estimates[28] of the amounts of brine inflow during heater operations which could have passed undetected through the collection system ranged up to ~10 liters for each array of seven canisters).

Table 2. Brine migration data obtained in the Project Salt Vault Experiment

	Room		Reference
	1	4	
Diameter of hole in salt, cm	30	30	28
Heated length of canister, cm	185	185	28
Water content of salt adjacent to canister prior to experiment, vol %	0.50	0.50	28
Heater power, kW/array	Ranged from 11 initially to 15 during final 150 days		28
Maximum temperature gradients in salt, °C/cm at temperature, °C	≤ 2 at $\sim$156	≤ 2 at $\sim$156	29[a]
Maximum temperature in salt, °C	200	200	28
Volume water collected prior to shutdown, liters/array	1.7	0.8	28
Volume water collected after shutdown, liters/array	9.0	12.8	28
Total water collected, liters/array	10.7	13.6	28
Maximum gamma dose to salt, rads	9.2×10^8	0	29[a]
Maximum stored radiation energy in salt, cal/g	1.0	0	29

[a]Estimated from information presented in ref. 28.

The explanation[28] offered for the marked release of brine during cooling of the salt was that the tangential stresses created by thermal expansion of the salt during heating were released upon cooling, allowing the trapped water in the salt to break free and enter the air gap space. This explanation seems substantially plausible to the author. A further suggestion might be that the brine was trapped on grain boundaries during heating and that release of tangential stresses allowed the grain boundaries to open sufficiently for the brine to escape to the air gap space. In support of these ideas, it should be noted that the thermal contraction of the salt at the surface of a cylindrical hole comparable in size to those in Rooms 1 and 4 of Project Salt Vault (Table 2) produces a decrease in area of $\sim$1.5 $cm^2/°C$.

Holdoway[2,3] conducted and reported petrofabric examinations of salt samples from a region adjacent to Array hole 2 in Room 1. This region was located in a direction outward from the periphery of the array of waste canisters. Evidence for brine migration within crystals was observed, but only a few trails crossed crystal boundaries. There was some evidence that droplets were spreading on grain boundaries. These observational results appear to be in support of the postulation that brine was trapped on grain boundaries during the heating phases of the Project Salt Vault Experiment.

3.2.2 Laboratory experiments of Bradshaw and Sanchez

Bradshaw and Sanchez[10] reported measurements of the rate of migration vs temperature of brine inclusions within natural single crystals obtained from the Carey mine at Hutchinson, Kansas. The temperatures employed ranged up to $\sim$250°C. The reported results of their rate measurements are reproduced in Fig. 1. The data scattered appreciably, and Jenks[24] assumed that the curve shown in Fig. 1 represents the maximum rates indicated by the data. The relationship between V and G_s along this curve is shown by Eq. (11)[24] (in other units):

$$\log V/G_s = 0.00656\ T - 0.6036, \qquad (11)$$

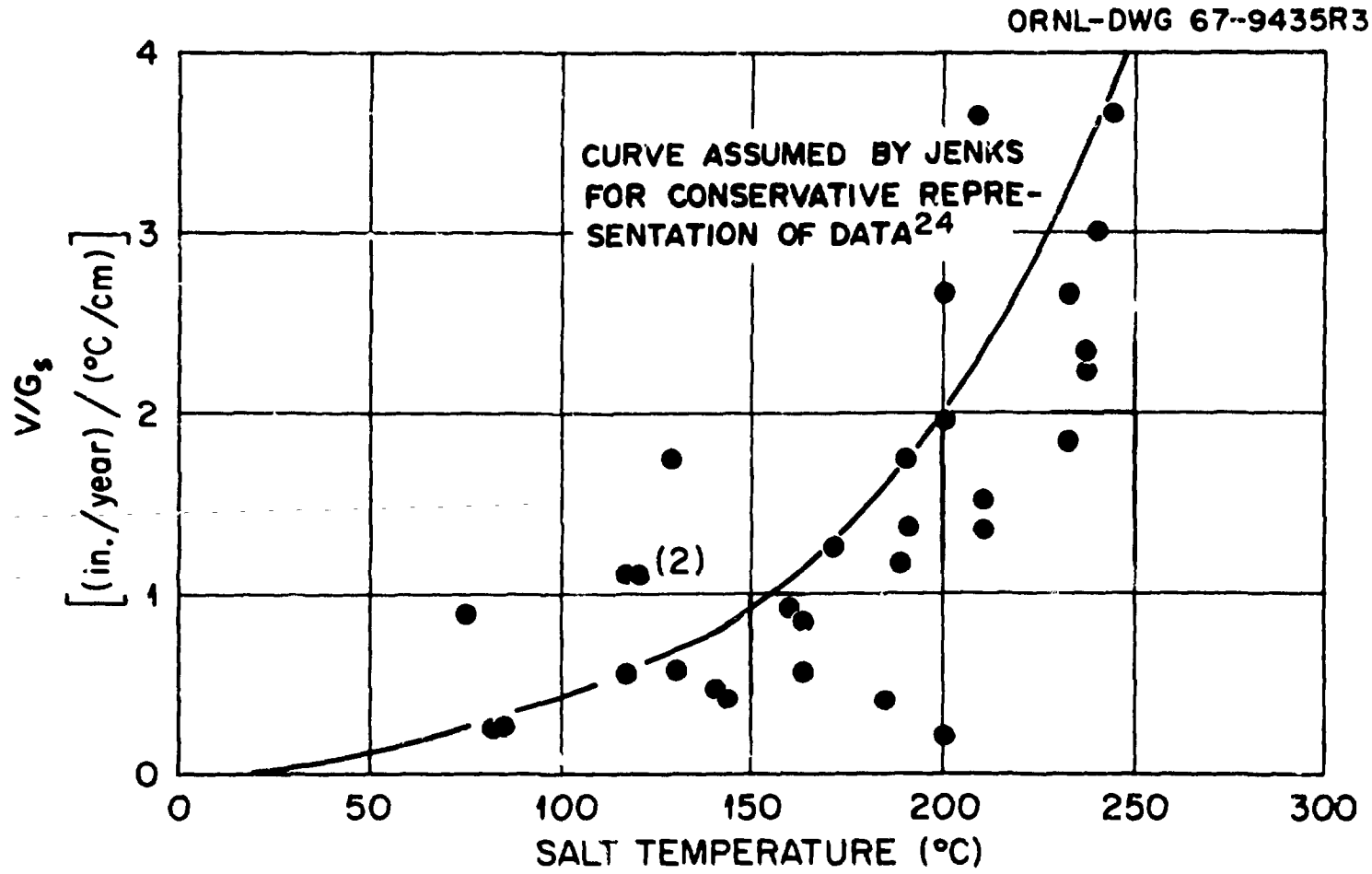

Fig. 1. Experimental data of Bradshaw and Sanchez for rates of migration of brine inclusions in Kansas salt.

where T is the temperature of the salt (°C) and V/G_s has the units (cm^2 $year^{-1}$ $°C^{-1}$).

Other relevant data that were reported by Bradshaw and Sanchez or can be inferred from their report[10] are summarized below:

1. Each of the single crystal samples employed was of the same size, ∿2.5 cm on a side.
2. The included brine cavities measured $\geq$ 2 mm but $\leq$ 10 mm on an edge.
3. Brine migration rates observed at temperatures >100°C were in the order of a few millimeters over a period of 1 or 2 days. These values are equivalent to rates >50 cm/year and to temperature gradients in the salt greater than ∿7°C/cm.
4. No brine migration rates were reported for temperatures <100°C.
5. The shape of inclusions was initially cubical but changed to oval during migration. No breakup was reported.

3.2.3 Laboratory experiments of Shor and Baes

Shor and Baes[30] have recently reported experimental observations of naturally occurring brine inclusions within a single crystal of salt from the Carey mine at Lyons, Kansas. One inclusion measured 150 x 100 μm; the other measured 65 x 65 μm. With a temperature of 100°C in the salt around the inclusions and with G_s = 35°C/cm, the former and latter inclusions migrated at rates, V, of 3.5 x 10^{-7} cm/sec and 2.0 x 10^{-7} cm/sec respectively. These results are compared with theoretical predictions in Sect. 3.3.1.

3.3 Comparisons Between Experimentally Determined and Theoretically Calculated Migration Rates

3.3.1 Data of Shor and Baes

I calculated V/V_{max} and K values [using Eqs. (11) and (8) and the concepts discussed in Sect. 3.1] for the experimental results and

conditions of Shor and Baes given in Sect. 3.2.3. Parameter values listed in columns 2, 3, 4, and 6 of Table 1 were used along with the experimental data in these calculations. For the larger and smaller droplets, respectively, values of 0.25 and 0.16 were found for the V/V_{max} ratio and 7.2×10^7 and 4.4×10^7 ergs/mole for K.

Values of K were also calculated for the experimental conditions of Shor and Baes, using Eq. (6), and the values for β and b that express the data for KCl reported by Cline and Anthony (i.e., $\beta = 1.85 \times 10^{14}$ erg-sec $mole^{-1}$ cm^{-1} and $b = 2.0 \times 10^6$ ergs/mole). The results, $K = 6.5 \times 10^7$ and 4.0×10^7 ergs/mole for the larger and smaller droplets respectively, are in very near agreement with those calculated from the experimental data. Overall consistency between theory and experiment is indicated, assuming that the relationship between K and V in naturally occurring NaCl crystals is approximately the same as that reported by Cline and Anthony for KCl at somewhat lower values of T and V.

3.3.2 Data of Bradshaw and Sanchez

Values for V/G_s at 50, 100, 150, and 200°C which were calculated using Eq. (11) (the Jenks fit to the experimental data of Bradshaw and Sanchez) are listed in the final column of Table 1, where they can be compared with the previously discussed theoretical values. In all cases, the theoretical values that were calculated with $\sigma = 0$ (Soret coefficient = 0) are lower than the results obtained experimentally; they range from ~48% of experimental at 50°C to ~65% of experimental at 150°C. The apparently low theoretical values might be a result, in part at least, of appreciable effects of thermal diffusion. This is very likely the case at 50°C since data available in the literature[21-23] indicate a σ value of $\sim -0.002°C^{-1}$ in concentrated NaCl solutions at this temperature. There is no known theoretical or experimental information which would enable reliable estimates of σ to be made at higher temperatures in the brine-inclusion solutions. However, it seems plausible to assume that they were equal to or greater than those at 50°C in the brine solutions.

Another possible explanation for the apparently low calculated values for V/G_s is that the estimated values for the diffusivity of NaCl in the brines solutions are too low by a small factor. Still another conceivable explanation is that the assumed value of 1.4 for G_ℓ/G_s was too low, which would be the case if the aspect ratio of the droplets had changed appreciably during migration. However, since Bradshaw and Sanchez report[10] only a small change (from cubical to oval), it is unlikely that the value of G_ℓ/G_s became significantly different from that for cubical droplets.

The comparisons between experimental and theoretical values of V/G_s indicate that there were no significant effects of kinetic potential (a rate-retarding potential discussed earlier) on the migration rates in those experiments where the rate values fell near the Jenks curve in Fig. 1. However, the results from the different experiments showed considerable scatter, with many of the points falling well below the Jenks curve. The occurrence of an appreciable kinetic potential seems to be the most reasonable explanation for the data scatter and the apparently low rate values. It is very likely that the value of this potential would depend strongly on the degree of perfection of the crystal and that the perfection varied appreciably from one experiment to another in the work of Bradshaw and Sanchez.[10] (Here, crystal perfection refers to the number and type of dislocations, number and type of impurities, and any prevailing stress within the crystal.) These properties could vary from one experiment to another, depending on the source, handling, rate of heating, size of the brine inclusion, and size of the crystal. In support of the idea that the kinetic potential was of importance in some of these experiments, it should be noted that values for the ratio, V/V_{max}, of 0.5 and 0.25 for the smallest (0.2-cm) droplets at G_s = 7°C/cm and at T = 150°C can be accounted for by K values of 2.2×10^8 and 3.3×10^8 ergs/mole respectively [see Eq. (8) and Table 1]. For comparison, the value of K that was calculated using Eq. (6) with $V = 1.6 \times 10^{-6}$ cm/sec (equivalent to 50 cm/year, the lowest value of V observed), and with values of β and b the same as those used previously in Sect. 3.3.1, was 2.9×10^8 ergs/mole.

In summary, the Jenks curve probably represents the maximum values of V/G_s that are likely to occur in the temperature range 50 to 200°C in crystals of bedded salt which are not subject to radiation or to externally imposed stresses during thermally induced migration. Effects of these parameters are discussed in Sects. 4 and 5.

4. EFFECTS OF STRESS ON BRINE MIGRATION IN SALT

4.1 Introduction

Both theoretical calculations and experimental results show that the solubility of NaCl in water increases with increasing pressure. Since brine migration within salt crystals is affected by solubility and solubility gradients (see Sect. 3), the possibilities of significant effects of stress (pressure) and stress gradients on brine migration in a repository need to be considered. In this section, as well as in Appendixes D-F, the theoretical information concerning pressure effects on the solubility of NaCl is reviewed and conceivable resulting effects on brine migration in a bedded salt repository are discussed. Three different cases with different effects of pressure are recognized and discussed separately. Brief descriptions of these are given in the paragraphs below.

Case 1. The solution within the cavity and the contacting salt are pressurized equally (e.g., when the inclusion that is completely filled with solution undergoes thermal expansion to pressurize the surrounding salt).

Case 2. The solid salt is stressed to a much greater extent than the contacting solution. One example of this case involves a situation in which an inclusion contains a low-pressure gas vapor bubble and the surrounding salt is subjected to a shear stress.[31] Another example, suggested by Boydell,[32] is one in which an externally stressed block of salt contains an open hole filled with solution.

Case 3. The salt surrounding a completely filled brine inclusion is subjected to a stress gradient. In practice in a repository, this case may not differ from Case 1.

4.2 Effects of Stress-Induced Changes in NaCl Solubility on Brine Migration

4.2.1 Case 1: Equal pressure on solution and salt

Considerations of the theoretical information on brine migration presented in Sect. 3.1 indicate that the principal effects of an increase in solubility on the maximum rate of thermal gradient-induced brine migration within a NaCl crystal will occur through an increase in the value of C_ℓ/C_s in Eq. (1). Thus, the indicated percentage increase in the migration rate would be equal to the percentage increase in the solubility of NaCl in the brine solution at the given temperature. The pressure-stress might also reduce the value of the kinetic potential, K, in Eq. (1); however, as discussed in Sect. 3.1, this reduction should have no significant effect on the maximum rate of brine migration.

Conceivably, a high pressure might also affect the value of the Soret coefficient, but no information on this is available. A pressure-induced increase in Case 1 solubility should have no significant effect on brine migration in the absence of a thermal gradient.

Appendix D shows that the theoretically predicted fractional increase in the Case 1 solubility of NaCl in NaCl solutions is small (e.g., $\leq$1.5 to 2% at a pressure of 500 atm and temperatures from 25 to 200°C). Experimental data on pressure effects on NaCl solubility at 25°C are available; the predicted and experimental results show good agreement (see Appendix D).

No comparable theoretical evaluations have been made of Case 1 pressure effects on NaCl solubility in the $MgCl_2$-NaCl brine solutions. These evaluations would require additional theoretical considerations and calculations in order to obtain estimates of the thermodynamic properties of these solutions of mixed electrolytes over the temperature and pressure range of interest. It is believed that the pressure effects would not be significantly greater than those in pure NaCl solutions, and that, at the extreme, the velocity of migration of droplets within crystals of bedded salt would not be increased by more than 5 to 10% by Case 1 pressure effects.

4.2.2 Case 2: Pressure on solid only

As described briefly in Sect. 4.1, the Case 2 pressure effect occurs in systems where the solid salt is stressed (pressurized) while the contacting fluid is either unpressurized or pressurized to a significantly lower value. As shown in Appendix E, the theoretically calculated value for the fractional increase in solubility of NaCl with increasing pressure is more than ten times that calculated for the systems in which the solution and contacting salt are pressurized equally (i.e., Case 1).

The effects of increased solubility in the Case 2 systems can be visualized as producing a solution adjacent to the stressed surface which is supersaturated in NaCl with respect to equilibrium solubility at the lower pressure prevailing over the solution. The supersaturated solution near the surface would lose salt by diffusion into the body of the solution as well as by precipitation on the nearest unstressed surfaces. These surfaces could be crystallites of NaCl formed and suspended within the solution.

Such Case 2 effects might occur with brine inclusions within salt crystals when the inclusions contain low-pressure gas vapor bubbles, and these effects could influence migration of the inclusions when there are gradients in the stresses in the salt around the inclusions. However, as stated below, it appears unlikely that low-pressure gas vapor bubbles will occur within brine inclusions which are located within the body of the salt. They might occur in salt located at the edge of an HLW or SURF emplacement cavity in the event that a portion of the liquid should escape into the cavity through temporary fractures or small blowouts which might develop when an inclusion approaches the surface of the cavity.[8,14,17]

Insufficient information is available to permit confident predictions regarding the fates of these two-phase inclusions after they are formed near the surface. However, it is known that the gas vapor phase will move down the temperature gradient as a result of reflux action.[8,14,17] At the same time, the liquid phase is moving up the temperature gradient. Depending on relative sizes of the two phases and other factors (such as the presence or absence of permanent gases, temperature gradients, and total size of the inclusion), either the gas vapor or liquid movement

may dominate and pull the other phase along or the two phases may separate and move in opposite directions.[14,17] Also, as indicated by recently reported observations,[31] the gas space within a two-phase droplet may be quickly shrunk and repressurized to a value near that on the surrounding salt. The process of movement to a free surface of the salt with loss of liquid and possible formation of a two-phase droplet could then be repeated until essentially all of the liquid has been released. While it would be interesting to have detailed information on the fates and behavior of brine inclusions at free surfaces, especially heated ones, it seems likely that the overall rates of migration of brine within a repository will not be significantly affected by this behavior.

As stated in Sect. 2, the fact that samples of bedded salt contain low-pressure gas vapor bubbles which persist to temperatures in excess of those prevailing within the undisturbed salt formation has not been satisfactorily explained. I believe that such bubbles do not initially exist in the undisturbed salt but are formed in some way, unspecified at present, after the lithostatic pressure on the salt has been relieved or during or after removal of the sample for examination. Yermakov[33] maintained that gas vapor bubbles form within laboratory specimens as a result of leakage of a portion of the included brine through the walls of the crystal, possibly through minute fractures. Additional experimental work is needed to satisfactorily explain the existence of such bubbles in samples and to determine whether they will occur in a repository.

Case 2 systems (not associated with brine inclusions) might occur in a salt repository in postulated accident situations in which the repository is flooded and when the pressures that develop on the flood liquid are less than those on the solid salt in contact with the liquid. Additional experimental information on the existence, nature, and action of surface stress will be needed in order to confidently predict the effects of stress, if any, on the behavior of the flooded system.

4.2.3 Case 3: Salt subject to a stress gradient

The pressure effects in this case will depend on the particular stress states that prevail around and within a brine inclusion. As implied in the introduction above, it seems likely that, for most conditions which can be visualized within the salt around a waste package, the thermal expansion* of the brine droplet will cause the stresses at the brine-salt interfaces to be directed from the solution into the salt. The Case 1 relationship would prevail under such conditions.

In the event that a large stress gradient exists in the salt around an inclusion and thermal expansion of the brine is not pressurizing the contacting salt, the stress effects on solubility may possibly be similar to those represented by Case 2. However, it seems more likely that no differences will exist among the stresses affecting solubility at the different brine-salt interfaces within a droplet because the hydraulic pressure exerted by the fluid on these interfaces cannot differ from one face to another.

5. EFFECTS OF STORED RADIATION ENERGY IN SALT ON BRINE MIGRATION

Gamma-ray energy can be stored in salt surrounding an emplaced waste package when the temperature of the salt is less than ~150°C.[35] The amount stored can be equivalent to several calories per gram after a period of several years following emplacement of the waste.[35] Thus, it is conceivable that this stored energy will have some effect on the solubility of the salt and, in turn, influence the migration rate of brine inclusions within the irradiated salt.**

---

*As an illustration of the large effects of thermal expansion of the droplet, please note that the pressure within the completely filled droplet increases by 12 to 13 bars per °C increase in the temperature range 50 to 100°C, assuming that the salt walls are rigid and do not undergo deformation.[34]

**A large gradient of stored energy could exist across a migrating inclusion since the salt that crystallizes on the cool side of the inclusion would be completely annealed with respect to stored energy.

The available experimental evidence from Project Salt Vault suggests that irradiation had no significant effects since the total amounts of brine collected from the irradiated and control arrays were approximately the same (see Sect. 3.2.1).

Experiments to determine the effects of stored energy on NaCl solubility should be performed as a means of establishing whether any appreciable radiation effects are likely to be encountered in a repository.

6. ESTIMATES OF RATES AND TOTAL AMOUNTS OF BRINE INFLOW TO WASTE EMPLACED IN BEDDED SALT

The amounts of brine that might migrate to HLW and SURF waste packages emplaced in bedded salt have been estimated by employing the emplacement models and results of temperature calculations reported by Llewellyn.[27] Three assumptions were made: (1) the salt contained 0.5 vol % brine inclusions, (2) the inclusions migrated at the maximum rates shown by Eq. (11), and (3) grain boundaries had no effect on the migration. The results of these estimates are mentioned here in order to illustrate the inflow volumes that might occur.

For HLW, the Llewellyn[27] model assumed 2.1 kW of 10-year-old waste contained within an 8-ft-high cylinder. The 17.7-in.-OD waste packages were emplaced at 150 kW/acre in a single row, on a 7.8-ft pitch, in the center of an open 18-ft room. The results of the present brine inflow estimates, in which the emplacement hole was assumed to be 2 ft in diameter and unbackfilled, indicated inflow rates of about 0.7 liter per year per package during the first 10 years following emplacement. The inflow rates then decreased, and the total inflow after 30 years was 12 liters.* The rate at 30 years was 0.18 liter/year.

The SURF model of Llewellyn assumed that 10-year-old PWR assemblies (550 W of thermal power over a 12-ft length) were emplaced at 60 kW/acre in a single row, on 5.1-ft centers, in the center of an open, 18-ft-wide

---

*No temperature calculations were made for more than 35 years following emplacement.

room. Each of the waste packages had an outside diameter of 17.7 in. The results of the estimates of brine inflow, in which the emplacement hole was again assumed to be 2 ft in diameter and unbackfilled, indicated a constant inflow rate of 0.035 liter per year per package for the first 35 years following emplacement.*

7. SUMMARY AND CONCLUSIONS

The available experimental and theoretical information on thermal gradient-induced brine migration in bedded salt was reviewed and analyzed. Data pertinent to the effects of stress and radiation in the solid salt and of pressure of the contacting brine on brine migration were also reviewed. The thermal-gradient information was then used as an aid and criterion in estimating the effects of other parameters on brine migration in a radioactive waste repository.

The thermal gradient-induced migration of brine droplets through solid KCl was studied in detail, both experimentally and theoretically, by Anthony and Cline at the General Electric Corporate Research Laboratories. They showed that the velocity of migration of a droplet through the solid KCl at a given temperature is dependent on several factors, including the concentration of salt in brine, the concentration gradient, the diffusivity of the salt within the liquid, and the undersaturation and supersaturation required at the dissolving and depositing interfaces respectively. The effects of these latter factors on brine migration are represented quantitatively in terms of a kinetic potential, K, which acts as a retardant to brine migration. The value of K is directly proportional to the velocity of migration, and the effect of a given K is inversely proportional to the dimension, L, of the droplet parallel to the thermal gradient.

The theoretical and experimental (with KCl) results of Anthony and Cline were used to correlate and explain the experimental results reported

---

*No temperature calculations were made for more than 35 years following emplacement.

by Shor and Baes for rates of brine migration at 100°C in naturally occurring crystals of bedded salt from Lyons, Kansas, and also the experimental results reported by Bradshaw and Sanchez for rates of migration of naturally occurring brine inclusions in crystals of bedded salt from Hutchinson, Kansas. The latter experiments employed temperatures ranging up to 250°C; however, only the data for temperatures $\leq$ 200°C are considered here.

It was concluded that the kinetic potential was of little importance in many of the experiments of Bradshaw and Sanchez and that a curve passing near the maximum of the observed values of V/G_s (migration velocity per unit temperature gradient) represents the maximum V/G_s values that result from thermal gradients in the bedded salt in a repository. This curve has the equation

$$\log V/G_s = 0.00656\ T - 0.6036,$$

where T is the temperature of the salt (°C) and the term V/G_s has the units ($cm^2\ year^{-1}\ °C^{-1}$).

It was also concluded that the retarding kinetic potential had considerable importance in many of the experiments of Bradshaw and Sanchez, and that differences between the values of the kinetic potential in these experiments accounted for most of the scatter observed in the V/G_s values. The kinetic potential was also found to be important in the experiments of Shor and Baes. Its significance in these cases was explained in terms of one or more of the following: the small sizes of the brine inclusions which were being investigated, the high temperature gradients and concomitant high migration velocities which were being employed, and the relatively high degree of perfection of the crystals that were being studied. As indicated above, the equation in the preceding paragraph is believed to represent the values of V/G_s when there are no appreciable effects of the retarding potential. Accordingly, this equation represents the maximum expected values of V/G_s, and the effect of a kinetic potential would be to reduce these values.

Consideration of the effects of stressing crystals of bedded salt on the migration properties of the brine inclusions within the crystals led to the conclusion that the most likely effects are a small fractional increase in the solubility of the salt within the liquid and a concomitant (and equal) fractional increase in the rate of the thermal gradient-induced migration of the brine. The application of high pressure could have the effect of reducing the value of the kinetic potential from that prevailing in the absence of the pressure, but this would have no effect on the maximum rates predicted by the equation shown earlier.

Estimates made by using theoretical and experimental information relative to pressure effects on solubility indicated that the fractional increase in the solubility of NaCl within aqueous solutions of NaCl would be in the range of 2 to 3% at a pressure of 1000 atm at 25°C, and less than this at higher temperatures (50, 100, 150, and 200°C) as well as at lower pressures. No comparable theoretical evaluations were made of the pressure effects on NaCl solubility in the $MgCl_2$-rich solutions known to comprise the brine that is included in bedded salt. Additional theoretical considerations and calculations would be required in order to obtain estimates of the thermodynamic properties of the solutions of mixed electrolytes over the temperature and pressure ranges of interest. The pressure effects would not be expected to be significantly greater than those encountered in the pure NaCl solutions; and, at the extreme, the rate of migration of the droplets within crystals of bedded salt would probably not be increased by more than 5 to 10% by pressure effects.

The presence of stored radiation energy within a salt crystal could affect the rate of brine migration within the crystal if the stored energy causes an increase in the solubility of the salt. However, results obtained in Project Salt Vault suggested that stored radiation energy had little, if any, effect on the rate of brine flow into the emplacement cavities in the salt. Since no direct information is available regarding the effects of stored energy on solubility of salt, experiments should be undertaken to obtain such information.

The greatest uncertainty associated with the prediction of rates of migration of brine into a waste emplacement cavity in bedded salt involves questions regarding the effects of the grain boundaries (within the

aggregates of single crystals which comprise a bedded salt deposit) on brine migration through the deposit. It is likely that grain boundary trapping will have important retarding effects on brine migration under the conditions which are expected to prevail with probable repository designs (viz., $G_s \leq 2°C$ maximum, impurities present on grain boundaries, and boundaries compressed by thermal expansion of the salt). It is also conceivable that the effects of grain boundaries will be opposite to those suggested above under some circumstances (e.g., when salt which has been heated is allowed to cool). Experimental results on brine migration obtained in Project Salt Vault suggested that most of the migrating brine was, in fact, trapped on grain boundaries during heating and was released during cooling when power failures occurred and after the heating had been terminated at the conclusion of the experiments. Of course, no comparable rapid cooling of the salt would occur in a waste repository in which the waste remains emplaced.

The results of some estimates of rates and total amounts of brine inflow to HLW and SURF waste packages emplaced in bedded salt were included in order to illustrate the inflow volumes that might occur in a repository. These estimates were made by using the results of temperature calculations reported by others[27] and by assuming that (1) the salt contained 0.5 vol % brine inclusions, (2) these inclusions migrated at the maximum rates shown by the equation presented in a preceding paragraph, and (3) that grain boundaries had no effect on the migration.

The results of the brine inflow estimates made in this study for 10-year-old HLW emplaced at 150 kW/acre indicated inflow rates starting at 0.7 liter/year and totaling 12 liters at 30 years after emplacement. (Temperature calculations did not extend beyond 35 years.) The estimates for 10-year-old PWR SURF emplaced at 60 kW/acre indicated a constant inflow rate of 0.035 liter/year for the first 35 years after emplacement (Temperature calculations did not extend beyond 35 years.)

8. APPENDIXES

Appendix A: Composition of Encapsulated Brine in Bedded Salt

A.1 Kansas Bedded Salt

Holser[7] reported experimental values (Table A.1) for the ratios of weights of Ca, Mg, Br, and SO_4 to Cl in the brine inclusions in salt samples taken from the mine at Hutchinson, Kansas, and also from a core from the Naval Air Station at the same location.* Ionic concentrations were not reported. He concluded that the brine inclusions were formed by the evaporation of seawater and that the concentration factor was about 60.**

Table A.1. Reported[a] concentration ratios in brine inclusions

Ratio	Weight basis	Mole basis[b]
Ca/Cl	0.000	0.000
Mg/Cl	0.231	0.337
Br/Cl	0.015	0.0067
SO_4/Cl	0.034	0.012

[a] W. T. Holser.[7]

[b] Derived from Holser's data.

Jenks and Bopp[5] reported (see Table A.2) concentrations for Na, Mg, Ca, and Br in brine collected from inclusions from samples of salt from the Carey Mine at Lyons, Kansas. The samples were obtained in each case by cleaving a NaCl crystal to expose a brine inclusion, collecting the

*These deposits, which are located about 20 miles from Lyons, Kansas, are thought to have substantially the same composition as those at Lyons.

**Holser further stated that the brine inclusions are probably unchanged samples of bitterns left behind in Permian time.

Table A.2. Results of analyses of samples of encapsulated brine from Lyons mine

Element	Amount of ion in sample: μg			Amount of ion in sample: M (25°C)			
	No. 1[a]	No. 2[b]	No. 3[c,d]	No. 1	No. 2	Average of No. 1 and No. 2	No. 3[d]
Na	44	19	-	1.89	1.92	1.905	-
Mg	50	23	31	2.03	2.21	2.12	1.6
Ca	1.3	0.7	-	0.03	0.03	0.03	-
Br	-	-	1.7	-	-	-	0.03 (0.04)[e]

[a]Sample volume = 0.00101 cm^3.

[b]Sample volume = 0.000428 cm^3.

[c]Sample volume = 0.000774 cm^3.

[d]Early sample.

[e]After adjustment for possible loss of sample, as indicated by results for magnesium.

brine in a calibrated capillary via capillary action, and immediately transferring the sample into an HCl solution in a small flask. Earlier samples that had been allowed to stand within the capillaries for long periods (~1 day) gave nonreproducible and inconsistent results.

The data in Tables A.1 and A.2 can be used to estimate the concentrations of each of the ions, including K, which are listed in the tables, if it is assumed that the ratios in Table A.1 apply to the samples in Table A.2 and that other elements were present in only trace concentrations. The procedure is described below.

The following relationship between the molar concentrations of cations and anions in the brines can be obtained from charge balance considerations:

$$2Mg^{2+} + Na^{+} + K^{+} + 2Ca^{2+} = Cl^{-} + Br^{-} + 2SO_4^{2-} . \qquad (A.1)$$

But, from the molar ratios in Table A.1,

$Cl^{-} = 2.967Mg^{2+}$,

$Br^{-} = 0.020Mg^{2+}$,

$SO_4^{2-} = 0.0037Mg^{2+}$.

Introducing these values into Eq. (A.1) and rearranging gives:

$$Na^{+} + K^{+} + 2Ca^{2+} = 1.061Mg^{2+} \text{ (molar concentrations)}. \qquad (A.2)$$

Now, substituting average values for Mg^{2+} and Ca^{2+} from Table A.2 (2.12 and 0.03 M, respectively) into Eq. (A.2) yields:

$$Na^{+} + K^{+} = 2.19 \text{ (molar concentrations)}. \qquad (A.3)$$

Since the average of the analytical value for Na^{+} was 1.91, the value for K^{+} was 0.28 M.

Values for molal concentrations were needed for use in considerations of solution properties at elevated temperatures. These were estimated by using the values for molar concentrations summarized in Table A.3, together with results of literature information for the molal concentrations of NaCl in NaCl-saturated $MgCl_2$ solutions at 25°C (shown in the

Table A.3. Summary of analytical and deduced values for concentrations in brine encapsulated in Kansas salt

	Concentration in brine[a]	
	M at 25°C	m
Mg	2.12	2.41
Na	1.91	2.16
K	0.28	0.32
Ca	0.03	0.034
Cl	6.29	7.15
Br	0.04	0.045
SO_4	0.078	0.089

[a] See text.

plot in Fig. A.1) and considerations of the probable density of the brine solution. Overall consistency between the various factors occurred when the density of the solution was assumed to be 1.22 (near the value which can be estimated for this solution)[36] and when the effects of the relatively small amounts of K, Ca, SO_4, and Br on the solubility of NaCl were assumed to be negligible in comparison with the effects of the larger amount of $MgCl_2$. The validity of the latter assumption is unknown, but it appears to be necessary in order to obtain consistency between the several factors mentioned above. Accordingly, the value of 1.22 (mentioned above) for the solution density at 25°C was used to determine the ratio of molal to molar concentrations in the brine solution.

Molal concentrations that were found using this ratio (i.e., 1.14) are listed in Table A.3.

A.2 New Mexico Bedded Salt

The brines included within the bedded salt at other potential sites for HLW or spent fuel have not been analyzed directly. The composition

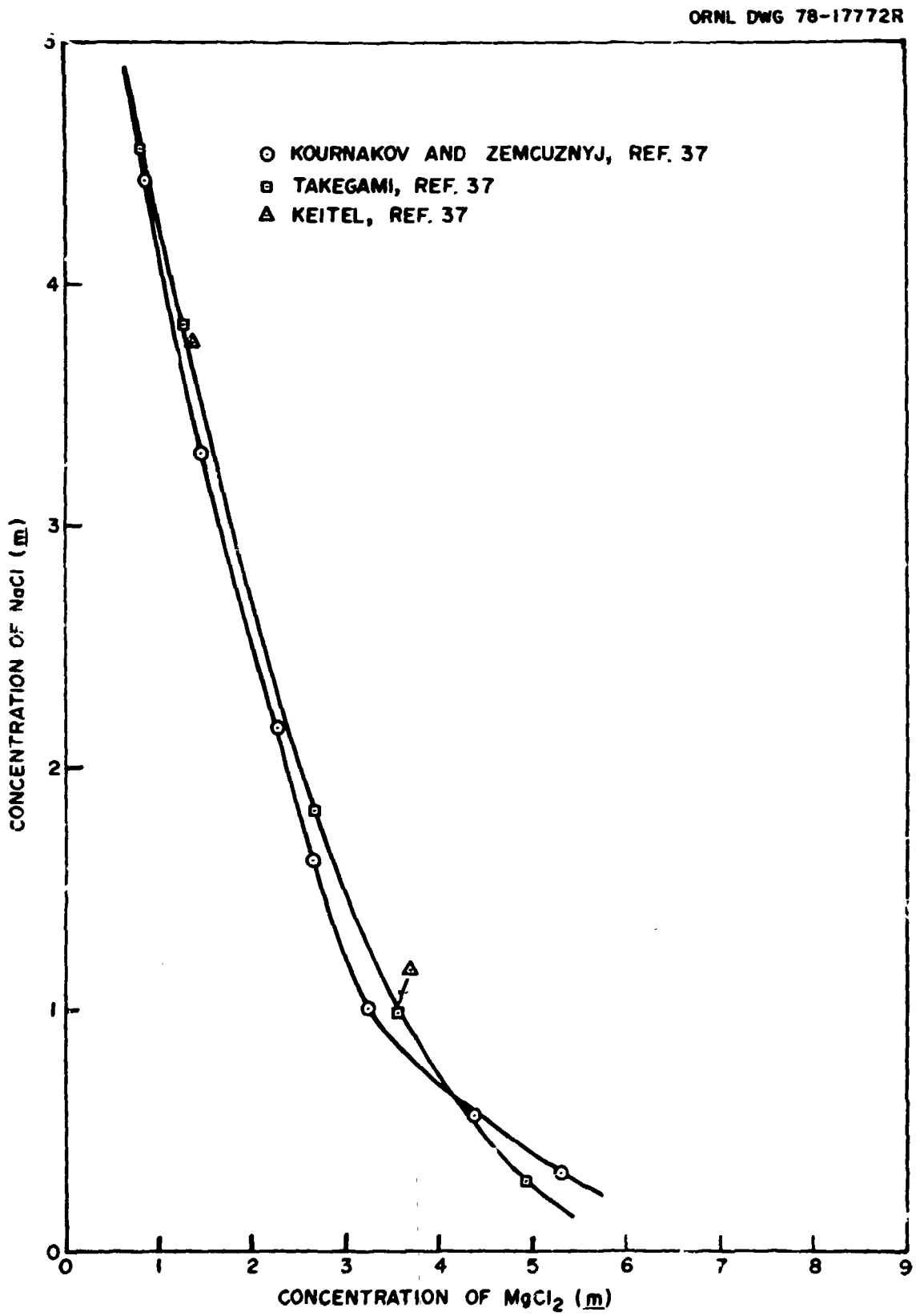

Fig. A.1. Concentration of NaCl in NaCl-saturated $MgCl_2$ solutions at 25°C.

of the WIPP Brine "A" (Table A.4) reported by Molecke[38] was based on the analyses of several brines from the McNutt potash-bearing region of the Salado. Not surprisingly, these brines were rich in potassium; the concentration in Brine A was 0.77 M at 25°C. The concentrations of Na, Mg, and Ca given for Brine A correspond to 1.8, 1.44, and 0.015 M at 25°C. These concentrations of Na and Ca are comparable to those found in the Kansas brines mentioned above; the Mg concentration is appreciably smaller.

Results of chemical analyses of core samples of salt from near the WIPP area have been reported by Beane and Popp[39] and by Molecke,[38] and information on brine composition can be inferred from their data.

The following is a summary of information given by Beane and Popp[39] for samples of salt taken from AEC Core 8 at nine different locations between depths of 2615 and 2821 ft. In general, the results showed that NaCl was the major constituent and anhydrite was a minor constituent of the samples. The results also indicated trace amounts of one or more of the following: polyhalite, iron oxide, K-feldspar, talc, chlorite, carnallite, bloedite, and quartz. The results of elemental analyses for K, Mg, and Ca were as follows: K, 0.03 wt % average, with maximum and minimum values of 0.09 and 0.01 wt %, respectively; Mg, 0.05 wt % average, with maximum values of 0.006 and 0.13 wt % in the soluble and insoluble portions of the samples, respectively; Ca, 0.62 wt % average, with maximum and minimum values of 1.3 and 0.14 wt %, respectively. The average weight losses on heating finely ground samples to 70, 200, and >400°C were 0.17, 0.18, and 0.47 wt % respectively. The three largest weight losses among the samples that were heated to >400°C were 1.66, 0.77, and 0.48 wt %. Samples from the same locations as these three also had appreciable amounts of insoluble material: 1.25, 0.92, and 0.91% respectively.

The results reported by Beane and Popp[39] for AEC Core 7 samples were in substantial agreement with those summarized above for Core 8 samples.

Table A.4. Compositions of WIPP brines A and B reported by Molecke[a]

Ion	Concentration [(mg/liter) ± 3%] Solution A	Solution B
Na^+	42,000	115,000
K^+	30,000	15
Mg^{2+}	35,000	10
Ca^{2+}	600	900
Fe^{3+}	2	2
Sr^{2+}	5	15
Li^+	20	-
Rb^+	20	1
Cs^+	1	1
Cl^-	190,000	175,000
SO_4^{2-}	3,500	3,500
$B(BO_3^{3-})$	1,200	10
HCO_3^-	700	10
NO_3^-	-	-
Br^-	400	400
I^-	10	10
pH (adjusted)	6.5	6.5
Specific gravity	1.2	1.2

[a]Data derived from ref. 38.

Pertinent inferences which can be drawn from the analytical results summarized above and from those presented in the Beane and Popp report[39] are:

1. The samples contained very little potassium, 0.032 wt % average.
2. The magnesium content of the samples was very low, averaging 0.006 wt % in the soluble portions. If the brine inclusions within the crystal boundaries of the salt contained $MgCl_2$ at a concentration of 2 M, the average amount of water within the inclusions was 0.13 wt %.
3. All of the calcium (average, 0.62 wt %) was in the form of anhydrite. No calcium was present as $CaCl_2$.

The WIPP Brine B which was reported by Molecke[38] (Table A.4) was based on the analysis of brine obtained by dissolving a portion of AEC Core 8 taken at a depth of 2725 ft. The reported composition is in substantial agreement with that expected on the basis of the results for Core 8 summarized above. In particular, it can be noted that the molar concentration of SO_4 exceeded that of calcium by about 60%, indicating that all of the calcium was present as $CaSO_4$.

A.3 Composition of White Material on Surfaces of Array Hole in Project Salt Vault

I have reviewed my notebook (A6580) records of October 3 to November 1, 1972, and find the following information relevant to this subject:

Scrapings of the surface of Hole 1 in PSV Room 1 at depths of 7.5, 9, and 10.5 ft were taken by Carey Salt personnel on September 24, 1972. These scrapings were analyzed at ORNL for Mg and Na by flame photometry and for other metals by spectrographic analysis. The results were as follows:

	Wt % of element				
Depth (ft)	Mg	Na	K	Ca	Other metals
7.5	8.7	20.5	1	0.35	Each <0.1
9.0	7.4	25.5	1	0.56	Each <0.1
10.5	7.4	24.5	0.07	0.39	Each <0.1

A portion of the 9-ft sample was analyzed for SO_4. The result showed 3.11%.

The Mg/Na ratio in each case is less than that measured for encapsulated brine. This suggests that some of the brine which entered the emplacement hole originated in dehydration of gypsum or other hydrated mineral.

Appendix B: Evaluation of the Quantity $(1/C_\ell)(\partial C_E/\partial T)$ in the Temperature Range 25 to 200°C in 2.41 m $MgCl_2$ Solutions

Values for the quantity $(1/C_\ell)(\partial C_E/\partial T)$ were needed in evaluations of the rates of brine migration in Kansas salt using Eq. (1):

$$V = \frac{C_\ell}{C_s}\frac{D}{RT}\left[\left(\frac{1}{C_\ell}\frac{\partial C_E}{\partial T} - \sigma\right)G_\ell RT - \frac{K}{L} - \frac{4\gamma\bar{V}_s}{XL}\right]. \qquad (1)$$

As set forth in the text (see Sect. 3.1), C_ℓ represents the saturation concentration of NaCl in the encapsulated brine in moles per liter of brine. However, the quantity $(1/C_\ell)(\partial C_E/\partial T)$ can also be written as $(1/C_\ell')(\partial C_\ell'/\partial T)$, where the prime sign indicates molal concentrations, since the concentration unit cancels out.

$$V = \frac{C_\ell}{C_s}\frac{D}{RT}\left[\left(\frac{1}{C_\ell'}\frac{\partial C_\ell'}{\partial T} - \sigma\right)G_\ell RT - \frac{K}{L} - \frac{4\gamma\bar{V}_s}{XL}\right]. \qquad (B.1)$$

The procedure followed was to first evaluate C_ℓ' in 2.41 m $MgCl_2$ solutions (see Appendix A) using literature data for the solubility of NaCl in $MgCl_2$ solutions of given concentrations over a range of $MgCl_2$ concentrations from ~1 to 5 m and over a range of solution temperatures to 200°C. These values of C_ℓ' in 2.41 m $MgCl_2$ solutions were then plotted vs temperature, and the values of $\frac{\partial C_\ell'}{\partial T}$ were determined from the plot.

The resulting values for C_ℓ', $\frac{\partial C_\ell'}{\partial T}$, and $\frac{1}{C_\ell'}\frac{\partial C_\ell'}{\partial T}$ are listed in Table B.1.

Table B.1. Results of evaluation of the quantity $\frac{1}{C_\ell'} \frac{\partial C_\ell'}{\partial T}$

Solution temperature (°C)	Concentration of NaCl in 2.41 m $MgCl_2$ solution, C_ℓ' (moles/kg H_2O)	$\frac{\partial C_\ell'}{\partial T}$ [mole (kg H_2O)$^{-1}$ °C^{-1}]	$\frac{1}{C_\ell'} \frac{\partial C_\ell'}{\partial T}$ (°C^{-1})
25	2.16	6.3×10^{-3}	2.92×10^{-3}
50	2.32	7.5×10^{-3}	3.23×10^{-3}
100	2.76	9.0×10^{-3}	3.36×10^{-3}
150	3.30	12.7×10^{-3}	3.85×10^{-3}
200	4.02	15.2×10^{-3}	3.78×10^{-3}

Appendix C: Evaluation of the Quantity C_ℓ/C_s in the Temperature Range 25 to 200°C in 2.41 m $MgCl_2$ Solutions

Values for the quantity C_ℓ/C_s were needed in evaluations of the rates of brine migration in Kansas salt using Eq. (1) of the text (see Sect. 3.1):

$$V = \frac{C_\ell}{C_s}\frac{D}{RT}\left[\left(\frac{1}{C_\ell}\frac{\partial C_E}{\partial T} - \sigma\right)G_\ell RT - \frac{K}{L} - \frac{4\gamma\bar{V}_s}{XL}\right].$$

As stated previously, C_ℓ is the saturation concentration of NaCl in the encapsulated brine and C_s is the concentration of NaCl in the solid salt, both in the units of moles per liter.

The evaluation procedure that was followed started with the values for C_ℓ' listed in Appendix B for the brine composition and temperatures of interest.

The relationship between molal and molar saturation concentrations of NaCl at 25°C in the Kansas brine solution was discussed in Appendix A. The relationships at higher temperatures were estimated by using the relationship at 25°C and assuming that the volumes of the solution increased with temperature due to thermal expansion and to the increases in the amount of salt in solution. The thermal expansion was assumed to be directly proportional to the thermal expansion of 5.5 m NaCl solution at saturation pressure.[40] The expansion resulting from the additional salt in solution was estimated by using a value of 24.5 cm^3/mole for the partial molal volume of NaCl in the brine solutions. Table C.1 lists the resulting values of C_ℓ, together with pertinent data used in evaluations of C_ℓ. The resulting values of C_ℓ were combined with the listed values of C_s to evaluate C_ℓ/C_s at temperatures of interest.

Table C.1. Results of evaluation of the quantity C_ℓ/C_s

Temperature (°C)	C_ℓ' (m)	Fractional increase in volume of solution due to increased amount of salt[a]	Relative density of 5.5 m NaCl solutions[b]	C_ℓ (M)	C_s[c] (M)	C_ℓ/C_s
25	2.16	1	1	1.91[d]	36.95	0.0517
50	2.32	1.003	0.989	2.02	36.82	0.0549
100	2.76	1.011	0.963	2.32	36.59	0.0634
150	3.30	1.020	0.931	2.66	36.36	0.0732
200	4.02	1.031	0.896	3.02	36.13	0.0836

[a] Increase with increasing temperature above 25°C, assuming that the partial molal volume at saturation is 24.5 ml per mole of NaCl.

[b] From values reported in ref. 40.

[c] Thermal expansion coefficient was assumed to have the value 1.30×10^{-4} °C/cm.

[d] From Appendix A.

Appendix D: Theoretical and Experimental Relationships Between Aqueous Solubility of NaCl and Pressure in Systems Having Equal Pressure on Solution and Solid, Case 1

D.1 Theoretical Relationship

The differential thermodynamic equation expressing the solubility-pressure relationshi, for this case is[32,41,42]

$$v_s \, dP = \bar{v} \, dP + RT \left(\frac{\partial \ell n \, a}{\partial m} \right)_{T,P} dm \, , \qquad (D.1)$$

where

m = molality of salt in solution, moles/kg H_2O;

P = pressure, atm;

v_s = molal volume of the solid salt, cm^3/mole;

$\bar{v}$ = partial molal volume of the dissolved salt at saturation, cm^3/mole;

a = activity of the dissolved salt;

T = temperature, °K;

R = gas constant (82.06 atm·cm^3/mole·°K).

Estimates of the effects of pressure on solubility of NaCl were made by using the integral of Eq. (D.1) as derived by Baes and Gable:[43]

$$\ell n \frac{m_2}{m_1} = \frac{(v_s - \bar{v})}{2RT} (P_2 - P_1) - \left[\left(\frac{\partial \ell n \gamma}{\partial m} \right)_{P_1} + \frac{1}{4RT} \left(\frac{d\bar{v}}{dm} \right) (P_2 - P_1) \right] (m_2 - m_1), \quad (D.$$

where γ represents the mean activity coefficient of the dissolved salt and the subscripts 1 and 2 refer to the lower- and higher-pressure conditions, respectively. The Baes and Gable derivation of this equation is reproduced in Appendix F. The principal assumptions were that each of the quantities $(\partial \bar{v}/\partial m)_P$ and $(v_s - \bar{v})$ is approximately constant at a given temperature.

The more approximate form of Eq. (D.2), shown in Eq. (D.3), was used for making estimates of the change in solubility of NaCl with pressure at temperatures of 25, 100, 150, and 200°C and at pressures of 1, 250, 500, and 1000 bars:

$$\ln \frac{m_2}{m_1} = \frac{1}{2RT} (v_s - \bar{v}) (\Delta P) - \left(\frac{\Delta\gamma}{\gamma\Delta m}\right)_{P_1} (m_2 - m_1)$$

$$- \frac{1}{4RT} \left(\frac{\Delta\bar{v}}{\Delta m}\right)_{P_1} (m_2 - m_1) \Delta P \ . \qquad (D.3)$$

The values for the variable quantities that were used in making these estimates are described and discussed in the subsections that follow.

D.2 Values for v_s, $\bar{v}$, $\frac{\Delta\gamma}{\gamma\Delta m}$, and $\frac{\Delta\bar{v}}{\Delta m}$ Used in Making Estimates of Pressure-Solubility Effects

D.2.1 Evaluation of v_s at room temperature and 1 atm pressure

The evaluation of v_s at room temperature (25°C) and 1 atm pressure is straightforward:

$$\frac{58.443 \text{ g/mole}}{2.165 \text{ g/cm}} = 26.99 \text{ cm}^3\text{/mole}.$$

The compressibility coefficient of solid NaCl is small (4.20×10^{-12} and 4.15×10^{-12} cm^2/dyne at 0 and 2 kbar, respectively),[43,44] and v_s can be regarded as approximately pressure independent, for present purposes, without introducing significant error into evaluations of pressure-solubility effects.

The volumetric thermal expansion coefficient, α, of solid NaCl is 1.175×10^{-4} and 1.425×10^{-4} °C^{-1} at zero pressure and 300 and 550°K, respectively.[43] Calculations using the average of these values (1.300×10^{-4} °C^{-1}) show that the solid salt will expand by 0.33, 0.98, 1.63, and 2.28% on heating from 25°C to 50, 100, 150, and 200°C respectively. The corresponding values of v_s are 27.08, 27.25, 27.43, and 27.61 cm^3/mole. The values of α at 2 kbar are only slightly less at the above temperatures (300 and 55°K) than those at zero pressure.[43]

D.2.2 Evaluation of $\bar{v}$ in saturated NaCl solutions

At room temperature and 1 atm pressure. Klotz[45] gives the following relationship for $\bar{v}$ at 25°C and 1 atm pressure:

$$\bar{v} = 16.6253 + 2.6607m^{\frac{1}{2}} + 0.2388m, \qquad (D.4)$$

where m is the molality of the solution in question. At saturation at 25°C and 1 atm, m = 6.146.[46] Then,

$\bar{v}$ = 24.69 cm^3/mole at 1 atm.

At 100, 150, and 200°C and saturation pressure. Haas[47] reported calculated values of $\bar{v}$ in NaCl solutions at temperatures between 80 and 325°C and at several different concentrations ranging up to saturation. The pressure over the saturated solutions was equal to the saturation vapor pressure at the given temperature. His values for saturated solutions at 100, 150, and 200°C were 24.52, 26.23, and 28.53 cm^3/mole. These values, along with the value at 25°C, are listed in Table D.1.

At elevated pressures. Values of $\bar{v}$ at elevated pressures can be calculated from density data, when available, by using Eq. (D.5):[48]

$$\bar{v} = \frac{M}{d} - \frac{(1000 + mM)(\partial d/\partial m)}{d^2}, \qquad (D.5)$$

where

m = concentration of solute, moles/kg H_2O;

M = molecular weight of NaCl, g/mole;

d = density of solution at temperature and pressure under evaluation, g/cm^3.

However, the accuracy of the available data[40] was not sufficient to determine whether an increase in the pressure above saturation pressure causes any significant change in the value of $\bar{v}$ from that prevailing at saturation pressure.

Table D.1. Values of $\bar{v}$ in saturated NaCl solution at several temperatures and at saturation pressure, and estimated values for $\Delta\bar{v}/\Delta m$ at concentrations near saturation

Temperature (°C)	NaCl concentration in saturated solution (m)	Pressure (atm)	Value of $\bar{v}$ in saturated NaCl solution (cm^3/mole)	Value of $\Delta\bar{v}/\Delta m$ (and range of m used in evaluation)
25	6.146	1	24.69[a]	0.775(6.146[a])
100	6.65	0.744	24.52	0.62(6.00-6.50)
150	7.22	3.44	26.23	2.94(6.50-7.00)
200	8.01	11.55	28.53[b]	1.66(7.50-8.00)

[a]Evaluated using Eq. (D.4). All values at other temperatures were obtained from values calculated and reported by Haas.[47]

[b]Haas[47] states that this value was calculated by extrapolation of the functions beyond their range.

D.2.3 Values of $\Delta\gamma/\gamma\Delta m$ in NaCl solutions near saturation concentration and at saturation pressure

Values for $\Delta\gamma/\Delta m$ were obtained using γ values for 5.5 and 6.0 m NaCl solutions reported by Silvester and Pitzer[49] (see Table D.2). Approximately the same values were assumed to prevail up to saturation at the given temperature. The values of γ in saturated solutions which were used have also been reported by Silvester and Pitzer.[46]

Table D.2. Values for $\Delta\gamma/\gamma\Delta m$ in saturated NaCl solutions at 25, 50, 100, 150, and 200°C

Parameter	NaCl concentration (m)	Temperature (°C)				
		25	50	100	150	200
γ	5.5	0.929	0.935	0.830	0.661	0.483
	6.0	0.989	0.990	0.965	0.680	0.491
	Saturation	1.008	1.022	1.915	0.724	0.515
$\Delta\gamma/\gamma\Delta m$		0.119	0.108	0.0765	0.0525	0.0311

D.2.4 Values of $\Delta\bar{v}/\Delta m$ in saturated NaCl solutions

Values of $\bar{v}\Delta/\Delta m$ at NaCl concentrations near saturation and at saturation pressure are listed in Table D.1. The sources of the data used in obtaining these values are included. As stated previously, the value of this quantity is assumed to be approximately independent of pressure in the range of pressures under consideration.

D.3 Calculated Values of the Ratio, m_2/m_1, of Equilibrium Concentrations of NaCl in Solution at Pressures P_2 and P_1

The results of calculations of m_2/m_1 using Eq. (D.3) are listed in Table D.3. The values for the several different factors used in making the calculations are also included. The m_2/m_1 values indicate that the solubility changes caused by high pressure on the solution and solid are less than $\sim$1.5% and less than $\sim$2.6% at 500 and 1000 atm respectively

Table D.3. Calculated values of the ratio of equilibrium concentrations of NaCl in solution, m_2/m_1, at pressures P_2 and P_1, and values for factors used in the calculations

Temperature (°C)	Initial pressure, P_1[a] (atm)	Initial concentration of NaCl[a] ($\underline{m}$)	ΔP (atm)	Difference between v_s and $\bar{v}$, $(v_s - \bar{v})$[a] (cm^3/mole)	$\frac{\Delta\gamma}{\gamma\Delta m}$ ($\underline{m}^{-1}$)[b]	$\frac{\Delta\bar{v}}{\Delta m}$[a] ($cm^3 \cdot kg/mole^2$)	m_2/m_1
25	1	6.146	250	2.30	0.119	0.775	1.0066
25	1	6.146	500	2.30	0.119	0.775	1.0131
25	1	6.146	1000	2.30	0.119	0.775	1.0259
100	0.74	6.65	250	2.55	0.0765	0.62	1.00686
100	0.74	6.65	500	2.55	0.0765	0.62	1.0124
100	0.74	6.65	1000	2.55	0.0765	0.62	1.0226
150	3.4	7.22	247	1.20	0.0525	2.94	1.00301
150	3.4	7.22	497	1.20	0.0525	2.94	1.00590
150	3.4	7.22	997	1.20	0.0525	2.94	1.00812
200	11.6	8.01	238	-0.92	0.0311	1.66	0.9977
200	11.6	8.01	488	-0.92	0.0311	1.66	0.9955
200	11.6	8.01	988	-0.92	0.0311	1.66	0.9911

[a] From Table D.1.

[b] From Table D.2.

D.4 Comparison Between Experimental and Theoretical Values for m_2/m_1 vs P at 25°C

Several investigators have reported measurements of the changes in the solubility of NaCl at 25°C resulting from overpressures at $\geq$250 atm.[50,51] The results, as summarized by Kaufmann,[50] showed m_2/m_1 equal to 1.0088, 1.0165, and 1.0305 at 250, 500, and 1000 atm respectively. These values are in near agreement with those obtained via theoretical calculations (listed in Table D.3). This agreement lends support to the validity of the calculation and estimation methods used in the present study.

Appendix E. Relationships Between Aqueous Solubility of NaCl and Pressure in Systems in Which Only the Solid Is Pressurized, Case 2

The thermodynamic equation expressing the solubility-pressure relationship in this case is:[52]

$$\int_{P_1}^{P_2} v_s \, dP = RT \ln a_2/a_1, \tag{E.1}$$

where the symbols are defined as noted previously in Appendix D. As before, subscripts 1 and 2 refer to the values of the parameters at the lower- and higher-pressure conditions respectively.

Since v_s is essentially independent of pressure, Eq. (E.1) can be rewritten as follows:

$$v_s(P_2 - P_1) = RT \ln a_2/a_1. \tag{E.2}$$

The activity in the NaCl solution is related to the mean activity coefficient, γ, and the concentration, m, by the equation

$$m\gamma = a^{\frac{1}{2}}. \tag{E.3}$$

Values for the ratio of activities, a_2/a_1, at several different temperatures and pressures were calculated using Eq. (E.2).* These calculated values are listed in Table E.1, along with values of $\gamma_2 m_2/\gamma_1 m_1$ which were calculated using Eq. (E.3).

These values, together with other information listed in the table, were used to calculate the corresponding values for m_2/m_1 using Eq. (E.4):

---

*Correns[53] reported a pressure-solubility relationship similar to the one shown in Eq. (E.2), except that Correns' equation is based on the ratio of concentrations rather than on the ratio of activities. As Table E.1 shows, there is a large difference between those two different quantities for NaCl solutions.

Table E.1. Calculated values for ratio of concentrations of NaCl in solution, m_2/m_1, when contacting salt is pressurized at P_2, starting at P_1

Temperature (°C)	Initial pressure (atm)	m_1 [c]	γ_1 [a]	ΔP (atm)	Molar volume of solid salt, v_s [b] (cm^3/mole)	Ratio of activity of solutions, a_2/a_1	$\frac{\gamma_2 m_2}{\gamma_1 m_1}$	$\frac{\Delta\gamma}{\gamma_1 \Delta m}$ [a]	Calculated ratio of NaCl concentrations in solution, m_2/m_1
25	1	6.146	1.008	250	26.98	1.32	1.15	0.119	1.08
25	1	6.146	1.008	500	26.97	1.74	1.32	0.119	1.17
25	1	6.146	1.008	1000	26.95	3.01	1.74	0.119	1.37
50	1	6.274	1.022	250	27.07	1.29	1.14	0.108	1.11
50	1	6.274	1.022	500	27.06	1.67	1.29	0.108	1.19
50	1	6.274	1.022	1000	27.03	2.77	1.67	0.108	1.38
100	1	6.680	0.915	250	27.24	1.25	1.12	0.077	1.08
100	1	6.680	0.915	500	27.34	1.56	1.25	0.077	1.16
100	1	6.680	0.915	1000	27.19	2.43	1.56	0.077	1.33
150	3.4	7.198	0.724	247	27.42	1.22	1.10	0.053	1.07
150	3.4	7.198	0.724	497	27.42	1.48	1.22	0.053	1.15
150	3.4	7.198	0.724	997	27.39	2.20	1.48	0.053	1.32
200	11.6	7.973	0.515	238	27.60	1.19	1.09	0.031	1.07
200	11.6	7.973	0.515	488	27.60	1.43	1.19	0.031	1.15
200	11.6	7.973	0.515	988	27.57	2.03	1.43	0.031	1.32

[a] Values taken from ref. 46.

[b] Reference information available in Appendix D.

[c] Values obtained from Table D.2.

$$\sqrt{\frac{a_2}{a_1}} = \left(\frac{m_2}{m_1}\right)\left(\frac{\gamma_2}{\gamma_1}\right) = m_1 Y\left(\frac{m_2}{m_1}\right)^2 + \left(\frac{m_2}{m_1}\right)\left(1 - m_1 Y\right), \tag{E.4}$$

where

$$Y = \frac{\Delta\gamma}{\gamma_1 \Delta m}, \tag{E.5}$$

and the assumed values of $\frac{\Delta\gamma}{\gamma_1 \Delta m}$ are those listed in Table D.2. These values are listed for convenience in Table E.1.

Equation (E.4) was derived by making use of the identities shown in Eqs. (E.6) and (E.7):

$$\gamma_2/\gamma_1 = 1 + \frac{\Delta\gamma}{\gamma_1} \tag{E.6}$$

and

$$\Delta m = \left(\frac{m_2}{m_1} - 1\right) m_1 . \tag{E.7}$$

As can be seen in Table E.1, the values for the concentration ratios are much greater than those calculated previously in Appendix D for systems in which the solution and solid are pressurized equally. An unpressurized solution at concentration, m_2, would obviously be unstable with respect to an unpressurized solid salt surface. Precipitation would probably occur rapidly on such a surface; however, as discussed previously (Sect. 4.2.2), this dissolution on a stressed surface and subsequent precipitation might affect brine movement in a salt repository in the unlikely situation where a Case 2 system is presumed to be present.

Appendix F: Derivation of Relationship for Effects of Pressure on the Solubility of NaCl

C. F. Baes, Jr., and R. W. Gable*

The condition for equilibrium is:

$$dG_s = d\bar{G}, \tag{F.1}$$

where G_s is the molar free energy of crystalline NaCl and $\bar{G}$ is the partial molal free energy of NaCl in the solution.

At constant temperature, one can write

$$\left(\frac{dG_s}{dP}\right)dP = \left(\frac{\partial \bar{G}}{\partial P}\right)_m dP + \left(\frac{\partial \bar{G}}{\partial m}\right)_P dm, \tag{F.2}$$

since G_s depends only on the pressure (P), while $\bar{G}$ depends on both the pressure and the molality (m) of NaCl in the solution.

The relationship of $\bar{G}$ to m is given by the following equation:

$$\bar{G} = \bar{G}^\circ + 2RT \ln (m\gamma), \tag{F.3}$$

where $\bar{G}^\circ$ is the free energy of NaCl in the standard state (a hypothetical ideal 1 molal solution) at the same temperature and pressure and γ is the mean activity coefficient. Here $\bar{G}^\circ$ depends only on P, while γ depends on both P and m. Appropriate differentiation of Eq. (F.3) gives

$$\left(\frac{\partial \bar{G}}{\partial m}\right)_P = 2RT\left[\frac{1}{m} + \left(\frac{\partial \ln \gamma}{\partial m}\right)_P\right] \tag{F.4}$$

and

$$\left(\frac{\partial \bar{G}}{\partial P}\right)_m = \bar{v} = \bar{v}^\circ + 2RT\left(\frac{\partial \ln \gamma}{\gamma P}\right)_m, \tag{F.5}$$

---

*Associate Professor of Chemistry, Davidson College, Davidson, North Carolina; presently a visiting member of the ORNL Chemistry Division.

where $\bar{v}$ and $\bar{v}^\circ$ are partial molal volumes of NaCl in the real solution and in the standard state. Also,

$$\frac{dG_s}{dP} = v_s, \tag{F.6}$$

where v_s is the molar volume of crystalline NaCl.

Substitution of Eqs. (F.4)-(F.6) into Eq. (F.2) yields

$$v_s \, dP = \bar{v} \, dP + 2RT \left[\frac{1}{m} + \left(\frac{\partial \ell n \, \gamma}{\partial m}\right)_P\right] dm,$$

which may be rearranged to give

$$d \, \ell n \, m = \left(\frac{v_s - \bar{v}}{2RT}\right) dP - \left(\frac{\partial \ell n \, \gamma}{\partial m}\right)_P dm. \tag{F.7}$$

While the derivative $\left(\frac{\partial \ell n \, \gamma}{\partial m}\right)_P$ can be evaluated at P = 1 atm below 100°C and near the saturation pressure of water above 100°C, an expression is needed for estimating this quantity at higher pressures. Since γ, like $\bar{G}$, depends on only P and m, it is possible to make use of the cross-differentiation condition:

$$\frac{\partial^2 \ell n \, \gamma}{\partial P \partial m} = \frac{\partial^2 \ell n \, \gamma}{\partial m \partial P}. \tag{F.8}$$

From Eq. (F.5),

$$\left(\frac{\partial \ell n \, \gamma}{\partial P}\right)_m = \frac{\bar{v} - \bar{v}^\circ}{2RT}; \tag{F.9}$$

and, since the partial molal volume in the the standard state does not depend on m, the combination of Eqs. (F.8) and (F.9) gives

$$\frac{\partial}{\partial P}\left(\frac{\partial \ell n \, \gamma}{\partial m}\right) = \frac{1}{2RT}\left(\frac{\partial \bar{v}}{\partial m}\right). \tag{F.10}$$

Integrating,

$$\left(\frac{\partial \ell n\ \gamma}{\partial m}\right)_P = \left(\frac{\partial \ell n\ \gamma}{\partial m}\right)_{P_1} + \frac{1}{2RT}\int_{P_1}^{P}\left(\frac{\partial \bar{v}}{\partial m}\right)_P dP. \qquad \text{(F.11)}$$

Here, P_1 is the reference pressure at which $\left(\frac{\partial \ell n\ \gamma}{\partial m}\right)_P$ is known. Equation (F.11) is the desired expression for $\left(\frac{\partial \ell n\ \gamma}{m}\right)_P$ in terms of P and $\bar{v}$.

Combining Eqs. (F.7) and (F.11) gives

$$d\ \ell n\ m = \left(\frac{v_s - \bar{v}}{2RT}\right)dP - \left(\frac{\partial \ell n\ \gamma}{\partial m}\right)_{P_1} dm - \frac{1}{2RT}\left[\int_{P_1}^{P_2}\left(\frac{\partial \bar{v}}{\partial m}\right)_P dP\ \ dm\right]. \qquad \text{(F.12)}$$

Introducing the approximation that $\left(\frac{\partial \bar{v}}{\partial m}\right)_P$ is a constant, $\frac{d\bar{v}}{dm}$,

$$d\ \ell n\ m \approx \left(\frac{v_s - \bar{v}}{2RT}\right)dP - \left(\frac{\partial \ell n\ \gamma}{\partial m}\right)_{P_1} dm - \frac{1}{2RT}\left(\frac{d\bar{v}}{dm}\right)(P - P_1)\ dm. \qquad \text{(F.13)}$$

Integrating,

$$\ell n\ \frac{m_2}{m_1} \approx \frac{1}{2RT}\int_{P_1}^{P_2}(v_s - \bar{v})\ dP - \left(\frac{\partial \ell n\ \gamma}{\partial m}\right)_{P_1}(m_2 - m_1)$$

$$- \frac{1}{2RT}\left(\frac{d\bar{v}}{dm}\right)\left[\int_{m_1}^{m_2} P\ dm - P_1(m_2 - m_1)\right]. \qquad \text{(F.14)}$$

The integral $\int_{m_1}^{m_2} P\ dm$ can be estimated satisfactorily by making the approximation that m varies linearly with P over the small range of m involved. Then,

$$\int_{m_1}^{m_2} P \, dm \simeq \frac{(P_2 + P_1)}{2} (m_2 - m_1). \qquad \text{(F.15)}$$

Substitution of Eq. (F.15) into Eq. (F.14) yields

$$\ln \frac{m_2}{m_1} \simeq \int_{P_1}^{P_2} \frac{(v_s - \bar{v})}{2RT} \, dP - \left[\left(\frac{\partial \ln \gamma}{\partial m} \right)_{P_1} + \frac{1}{4RT} \left(\frac{d\bar{v}}{dm} \right) (P_2 - P_1) \right] (m_2 - m_1). \qquad \text{(F.16)}$$

Neglecting any change of $v_s - \bar{v}$ with P, one obtains:

$$\ln \frac{m_2}{m_1} \simeq \left(\frac{v_s - \bar{v}}{2RT} \right) (P_2 - P_1) - \left[\left(\frac{\partial \ln \gamma}{\partial m} \right)_{P_1} + \frac{1}{4RT} \left(\frac{d\bar{v}}{dm} \right) (P_2 - P_1) \right] (m_2 - m_1). \qquad \text{(F.17)}$$

With $(v_s - \bar{v})$, $(\partial \ln \gamma / \partial m)$, and $(d\bar{v}/dm)$ known at T and the reference pressure, P_1, this equation can be solved by iteration for m at another pressure P.

9. REFERENCES

1. W. A. Schneider, H. Hughes, and E. C. Robertson, Thermal Conductivity to 300°C of Natural Salt, U.S. Geological Survey Technical Letter (April 1962).

2. K. A. Holdoway, Petrofabric Changes in Heated and Irradiated Salt from Project Salt Vault, Lyons, Kansas, ORNL/Sub-3484/4 (June 1972).

3. K. A. Holdoway, "Behavior of Fluid Inclusions in Salt During Heating and Irradiation," pp. 303-12 in Fourth Symposium on Salt, Vol. 1, Northern Ohio Geol. Soc., Inc., Cleveland, Ohio (1974).

4. R. M. Dreyer, R. M. Garrels, and A. L. Howland, "Liquid Inclusions in Halite as a Guide to Geologic Thermometry," Am. Mineral. 54, 26 (1949).

5. G. H. Jenks and C. D. Bopp, "Composition of Encapsulated Brine in Salt," pp. 216-18 in Radioactive Waste Repository Project Annual Progress Report for Period Ending September 30, 1972, ORNL-4824 (December 1972).

6. D. W. Powers, S. J. Lambert, S. E. Shaffer, and L. R. Hill (Eds.), Draft Site Characterization Report for the Waste Isolation Pilot Plant (WIPP) Southeastern New Mexico, SAND78-1596, Vol. II (August 1978), pp. 7-56 and Table 7.14.

7. W. T. Holser, "Chemistry of Brine Inclusions in Permian Salt from Hutchinson, Kansas," pp. 86-95 in Symposium on Salt, Northern Ohio Geol. Soc., Inc., Cleveland, Ohio (1963).

8. W. R. Wilcox, Removal of Liquid Inclusions from Solution-Grown Crystals, Aerospace Report No. TR-1001 (9230-03)-5 (April 1967).

9. W. R. Wilcox, "Removing Inclusions from Crystals by Gradient Techniques," Ind. Eng. Chem. 60, 13-23 (1968).

10. R. L. Bradshaw and F. Sanchez, "Brine Migration Studies," p. 32 in Health Phys. Div. Annu. Prog. Rep. July 31, 1968, ORNL-4316 (October 1968).

11. T. R. Anthony and H. E. Cline, "Thermal Migration of Liquid Droplets Through Solids," J. Appl. Phys. 42, 3380 (1971).

12. H. E. Cline and T. R. Anthony, "Vaporization of Liquid Inclusions in Solids," Phil. Mag. 24, 1483 (1971).

13. H. E. Cline and T. R. Anthony, "The Thermomigration of Liquid Droplets Through Grain Boundaries in Solids," Acta Metall. 19, 491 (1971).

14. T. R. Anthony and H. E. Cline, "The Thermomigration of Biphase Vapor-Liquid Droplets in Solids," Acta Metall. 20, 247 (1972).

15. H. E. Cline and T. R. Anthony, "Effects of the Magnitude and Crystallographic Direction of a Thermal Gradient on Droplet Migration in Solids," J. Appl. Phys. 43, 10 (1972).

16. T. R. Anthony and H. E. Cline, "The Stability of Migrating Droplets in Solids," Acta Metall. 21, 117 (1973).

17. W. R. Wilcox, "Anomalous Gas-Liquid Inclusion Movement," Ind. Eng. Chem. 61, 76-77 (1969).

18. Kuo-Hung Chen and W. R. Wilcox, "Boiling and Convection During Movement of Solvent Inclusions in Crystals," Ind. Eng. Chem. 11, 563-65 (1972).

19. E. C. Stoner, "The Demagnetizing Factors for Ellipsoids," Phil. Mag. 36, 816 (1945).

20. W. A. Tiller, "Migration of a Liquid Zone Through a Solid: Part I," J. Appl. Phys. 34, 2757 (1963).

21. C. C. Tanner, "The Soret Effect," Trans. Faraday Soc. 23, 75 (1927).

22. L. G. Longsworth, "The Temperature Dependence of the Soret Coefficient of Aqueous Potassium Chloride," J. Phys. Chem. 69, 1557 (1957).

23. H. J. B. Tyrrell, "Thermal-Diffusion Phenomena in Electrolytes and the Constants Involved," in Electrochemical Constants, National Bureau of Standards Circular 524, U.S. Department of Commerce (1953).

24. G. H. Jenks, Radiolysis and Hydrolysis in Salt-Mine-Brines, ORNL-TM-3717 (March 1972).

25. N. A. Gjostein and F. N. Rhines, "Absolute Interfacial Energies of [001] Tilt and Twist Grain Boundaries in Copper," Acta Metall. 7, 319 (1959).

26. F. Seitz, The Modern Theory of Solids, pp. 96-98, McGraw-Hill, New York, 1940.

27. G. H. Llewellyn, Prediction of Temperature Increases in a Salt Repository Expected from the Storage of Spent Fuel or High-Level Waste, ORNL/ENG/TM-7 (April 1978).

28. R. L. Bradshaw and W. C. McClain (Eds.), Project Salt Vault: A Demonstration of the Disposal of High Activity Wastes in Underground Salt Mines, ORNL-4555 (April 1971).

29. G. H. Jenks and C. D. Bopp, Storage and Release of Radiation Energy in Salt in Radioactive Waste Repositories, ORNL-TM-4449 (January 1974).

30. A. J. Shor and C. F. Baes, Jr., Letter to G. H. Jenks, "Geological Disposal Technology Program Progress Report for October 1978," dated Nov. 1, 1978.

31. D. W. Powers, S. J. Lambert, S. E. Shaffer, and L. R. Hill (Eds.) Draft Site Characterization Report for the Waste Isolation Pilot Plant (WIPP) Southeastern New Mexico, SAND78-1596, Vol. II (August 1978), pp. 7-64 and Plate 7.40.

32. H. C. Boydell, "A Discussion on Metasomatism and the Linear Force of Growing Crystals," Econ. Geol. 21, 1-55 (1926).

33. N. P. Yermakov, "Research on the Nature of Mineral-Forming Solutions," ed. by E. Roedder (transl. by V. P. Sokoloff), International Series of Monographs in Earth Sciences, Vol. 22, Chaps. 3, 6, Pergamon, New York, 1965.

34. R. W. Potter II, "Pressure Corrections for Fluid-Inclusion Homogenization Temperatures Based on the Volumetric Properties of the System NaCl-H_2O," J. Res. U.S. Geog. Surv. 5, 603-7 (1977).

35. G. H. Jenks and C. D. Bopp, Storage and Release of Radiation Energy in Salt, ORNL-5058 (October 1977).

36. J. L. Haas, Jr., and R. W. Potter II, "The Measurement and Evaluation of PVTX Properties of Geothermal Brines and the Derived Thermodynamic Properties," pp. 604-13 in Proceedings of the Seventh Symposium on Thermophysical Properties, ed. by Ared Cezairliyan, American Society of Mechanical Engineers, 1977.

37. W. F. Linke, Solubilities, Inorganic and Metal-Organic Compounds, Vol. 2, 4th ed. (A Revision and Continuation of the Compilation Originated by A. Seidell), p. 489, American Chemical Society, Washington, D.C., 1965.

38. M. A. Molecke, Letter to Distribution, "Revised Representative Brines/Solutions for WIPP Experimentation," dated Oct. 8, 1976. [According to Molecke, these analyses are quoted by R. G. Dosch and A. W. Lynch, Interactions of Radionuclides with Geomedia Associated with the Waste Isolation Pilot Plant Site, SAND78-02-97 (June 1978). M. A. Molecke, private communication to G. H. Jenks, Nov. 15, 1978.]

39. R. E. Beane and C. J. Popp, Chemical, Mineralogical, and Thermogravimetric Analysis of Selected Core Samples from Carlsbad, New Mexico, ORNL/Sub-3673/3 (June 1975).

40. R. W. Potter II and D. L. Brown, The Volumetric Properties of Aqueous Sodium Chloride Solutions from 0° to 500°C at Pressures up to 2000 bars Based on a Regression of Available Data in the Literature, Geological Survey Bulletin 1421-C (1977).

41. I. M. Klotz, Chemical Thermodynamics, pp. 253-54, Prentice-Hall, New York, 1950.

42. C. F. Baes Jr., and R. W. Gable, ORNL Chemistry Division, private communication (November 1978); see Appendix F.

43. H. Spetzler, C. G. Sammis, and R. J. O'Connell, "Equation of State of NaCl: Ultrasonic Measurements to 8 kbar and 800°C and Static Lattice Theory," Phys. Chem. Solids 33, 1727-50 (1972).

44. D. W. Kaufmann, Sodium Chloride, p. 591, Reinhold, New York, 1960.

45. I. M. Klotz, Chemical Thermodynamics, p. 195, Prentice-Hall, New York, 1950.

46. L. F. Silvester and K. S. Pitzer, "Thermodynamics of Electrolytes. 8. High-Temperature Properties, Including Enthalpy and Heat Capacity, with Application to Sodium Chloride," J. Phys. Chem. 81, 1822-28 (1977).

47. J. L. Haas, Jr., Thermodynamic Properties of the Coexisting Phases and Thermomechanical Properties of the NaCl Component in Boiling NaCl Solutions, Geological Survey Bulletin 1421-B (1976).

48. I. M. Klotz, Chemical Thermodynamics, pp. 202-3, Prentice-Hall, New York, 1950.

49. L. F. Silvester and P. S. Pitzer, Thermodynamics of Geothermal Brines, I. Thermodynamic Properties of Vapor-Saturated NaCl(aq) Solutions from 0-300°C, LBL-4456 (January 1976).

50. D. W. Kaufmann, Sodium Chloride, p. 617, Reinhold, New York, 1960.

51. G. F. Becker and A. L. Day, "Note on the Linear Force of Growing Crystals," J. Geol. 24, 313-33 (1916).

52. C. F. Baes, Jr., ORNL Chemistry Division, private communication (November 1978).

53. C. W. Correns, "Growth and Dissolution of Crystals Under Linear Pressure," Discuss. Faraday Soc. 5, 267-71 (1949).

ORNL-5526
Dist. Category UC-70

INTERNAL DISTRIBUTION

1. C. F. Baes, Jr.
2. R. E. Blanco
3. J. O. Blomeke
4. G. D. Brunton
5. W. D. Burch
6. H. C. Claiborne
7. L. R. Dole
8. R. B. Fitts
9. R. W. Gable
10. R. W. Glass
11-40. G. H. Jenks
41. R. K. Kibbe
42. K. A. Kraus (consultant)
43. T. F. Lomenick
44. A. L. Lotts
45-64. W. C. McClain
65. J. G. Moore
66. E. Newman
67. K. J. Notz
68. H. A. Pfuderer
69. A. S. Quist
70. A. J. Shor
71-74. Laboratory Records
75. Laboratory Records, R.C.
76-77. Central Research Library
78. ORNL — Y-12 Technical Library Document Reference Section
79. ORNL Patent Section

EXTERNAL DISTRIBUTION

Argonne National Laboratory, 9700 South Cass Avenue, Argonne, IL 60439
80. A. M. Friedman
81. L. J. Jardine

Associated Universities, Inc., Brookhaven National Laboratory, Upton, NY 11973
82. P. W. Levy

Atomic Energy of Canada Limited, Whiteshell Nuclear Research Establishment, Pinawa, Manitoba, ROE 1LO CANADA
83. P. Sargent
84. H. Y. Tammemagi

Battelle Memorial Institute, Office of Nuclear Waste Isolation, 505 King Avenue, Columbus, Oh 43201
85-89. N. E. Carter
90. W. A. Carbiener
91. J. O. Duguid
92. J. F. Kircher
93. D. P. Moak
94. G. E. Raines
95. R. A. Robinson

Battelle Pacific Northwest Laboratories, P.O. Box 999, Richland, WA 99352
96. J. E. Mendel
97. R. J. Serne
98. A. M. Platt

Clark University, Department of Government and Geography, Worchester, MA 01610
99. R. Kasperson

CNEN-CSN CASACCIA, Laboratorio Rafitui Radioattivi, c.p. 2400, 0010 Rome, ITALY
100. W. Bocola

Cornell University, Department of Physics, Ithaca, NY 14935
101. R. O. Pohl

CSIRO, Division of Environmental Studies, P.O. Box 821, Canberra City, AUSTRALIA
102. J. R. Philip

Elkraft, Power Company Ltd., Parallelvej 18, DK-2800, Lyngby, DENMARK
103. F. Hasted

Florida State University, Department of Oceanography, Tallahassee, FL 32306
104. J. W. Winchester

Geological Society of America, Inc., 3300 Penrose Place, Boulder, CO 80301
105. J. C. Frye

Geological Survey of Canada, Regional & Economic Geology Division, 601 Booth Street, Ottawa, K1A OE8 CANADA
106. B. Sanford

Institut für Tieflagerung, Wissenschaftliche Abteilung, 3392 Clausthal-Zellerfeld, WEST GERMANY
107. K. Kühn
108. F. Oesterle

Law Engineering Testing Company, 2749 Delk Road, S.E. Marietta, GA 30069
109. J. G. LaBastie

Louisiana State University, Institute for Environmental Studies, P.O. Drawer J.D., Baton Rouge, LA 70803
110. J. D. Martinez

National Research Council, Committee on Radioactive Waste Management JH826, 2101 Constitution Avenue, Washington, DC 20418
111. J. T. Holloway

Netherlands Energy Research Foundation, Technical Services Department, Westernduinweg 3, Petten, NETHERLANDS
112. J. Hamstra

New York University Medical Center, Department of Environmental Medicine, New York, NY 10016
113. M. Eisenbud

Nuclear Regulatory Commission, Washington, DC 20555
114. D. M. Roher

Oak Ridge Associated Universities, Institute for Energy Analysis, Oak Ridge, TN 37830
115. A. M. Weinberg

OECD-Nuclear Energy Agency, 38 boulevard Suchet, Paris, FRANCE
116. F. Gera

Ohio State University, Department of Metallurgical Engineering, Columbus, OH 43210
117. R. W. Staehle

Pennsylvania State University, Department of Hydrogeology, University Park, PA 16802
118. R. R. Parizek

Pennsylvania State University, Materials Research Laboratory, University Park, PA 16802
119. J. V. Biggers
120. D. M. Roy

PPG Industries, Inc., Glass Research Center, Box 11472, Pittsburgh, PA 11472
121. F. M. Ernsberger

RE/SPEC Inc., P.O. Box 725, Rapid City, SD 57701
122. P. F. Gnirk
123. W. B. Krause

Sandia Laboratories, P.O. Box 5800, Albuquerque, NM 87185
124. F. A. Donath - 5413
125. L. R. Hill - 4511
126. R. C. Lincoln - 5444
127. M. A. Molecke - 1141
128. A. R. Sattler - 1141
129. H. C. Schefelbine - 4541
130. W. D. Weart - 1140

233 Virginia, Ponca City, OK 74601
131. D. A. Shock

Stanford University, Department of Geology, Stanford, CA 94305
132. K. B. Krauskopf

University of Arizona, Department of Hydrology and Water Resources
Tucson, AZ 85721
133. S. N. Davis

University of California, Berkeley, California 94720
134. Dr. Olander

University of California, Department of Nuclear Engineering, Berkeley,
CA 94720
135. T. H. Pigford

University of California, Lawrence Livermore Laboratory, P.O. Box 8,
Mail Stop L-90, Livermore, CA 94550
136. B. Davis

University of California, Lawrence Livermore Laboratory, Livermore,
CA 94550
137. H. C. Heard

University of California, Los Alamos Scientific Laboratory, P.O. Box
1663, Los Alamos, NM 87545
138. G. A. Cowan

University of Florida, Department of Nuclear Engineering, Gainsville,
FL 32611
139. J. A. Wethington

University of New Mexico, Department of Geology, Albuquerque, NM 87131
140. D. G. Brookins

University of Pittsburgh, Department of Physics and Astronomy, Pittsburgh,
PA 15260
141. B. L. Cohen

University of Texas, Acting Director, Marine Science Institution, P.O. Box 799, University Station, Austin, TX 78712
142. P. T. Flawn

University of Texas at Austin, College of Engineering, Austin, TX 78712
143. E. F. Gloyna

U.S. Department of Energy, Oak Ridge Operations, Radioactive Waste Management Division, Oak Ridge, TN 37830
144. D. E. Large

U.S. Department of Energy, Oak Ridge Operations, Energy Research and Development Division, Oak Ridge, TN 37830
145. Office of Assistant Manager

U.S. Geological Survey, 12201 Sunrise Valley Drive, Reston, VA 22092
146. G. D. DeBuchananne
147. E. W. Roedder
148. D. B. Stewart

U.S. Geological Survey, Experimental GChem & Mineralogy, 345 Middlefield Road, MS 18, Menlo Park, CA 94025
149. R. W. Potter, II

Vanderbilt University, Department of Environmental Engineering, Nashville, TN 37235
150. F. L. Parker

151-483. Given distribution as shown in TID-4500 under Nuclear Waste Management Category

☆U.S. GOVERNMENT PRINTING OFFICE: 1979-640-079-103